R-14-21

Modelling of the mechanical interaction between the buffer and the backfill in a KBS-3V repository

Updated design of backfill and deposition hole

Lennart Börgesson, Clay Technology AB

Jan Hernelind, 5T Engineering AB

April 2014

Svensk Kärnbränslehantering AB
Swedish Nuclear Fuel
and Waste Management Co

Box 250, SE-101 24 Stockholm
Phone +46 8 459 84 00

ISSN 1402-3091
SKB R-14-21
ID 1392113

Modelling of the mechanical interaction between the buffer and the backfill in a KBS-3V repository

Updated design of backfill and deposition hole

Lennart Börgesson, Clay Technology AB

Jan Hernelind, 5T Engineering AB

April 2014

Keywords: Buffer, Backfill, Bentonite, Interaction, Swelling, Deposition hole, Modelling, Finite element.

Abstract

Swelling of the buffer towards the backfill and the pellet filled bevel may lead to a loss in density of the buffer material that is unacceptable. This interaction between buffer and backfill has earlier been investigated and modelled in several projects. The results showed that the combination of a water saturated buffer that swells against a dry backfill is the most critical case and have led to conclusions about the design. However, after the referred calculations were done the design has been modified and a bevel in the floor at the deposition hole introduced in order to simplify the installation of the canister.

In order to further study the buffer / backfill interaction the following two studies have been made:

1. Bevel, updated backfill block geometries and pellet filling in top of the deposition hole instead of half-block.
2. Half-block in top of the deposition hole as in the reference design.

In the first study three types of calculations have been performed with the finite element code Abaqus. In these calculations the buffer has been modelled as completely water saturated with free access to water. The backfill has been modelled in different ways:

- Dry case
  - Dry backfill with different properties of the pellet fillings.
  - Dry backfill without pellet filling at the roof.
- Wet case
  - Completely water saturated backfill with bevel in the floor.

However, the complicated geometries and material models and the large displacements that occurred in some models entailed considerable modelling problems mainly due to lack of convergence. The problems led to that simplified numerical models and (in some cases) not completed calculations had to be used for the evaluation of the studies. In spite of the problems enough results were obtained in order to draw the conclusions presented in the study.

The following main conclusions could be drawn:

Dry case

The stiffness and thickness of the pellet filling are the dominating properties regarding the influence on the upwards swelling and the subsequent density loss of the buffer. The results show that the design with pellet filling in top of the deposition hole does not fulfil the requirements neither for uncompacted pellet filling nor for compacted pellet filling.

The influence of the properties of the pellet filling at the roof is not very strong and the calculations imply that loose filling is acceptable but also that the pellet filling is needed and cannot be excluded.

The influence of the backfill block section in the tunnel (and thus the horizontal joints between the blocks) is rather strong especially for those cases that are acceptable. It is thus important to learn more about the joint properties.

Wet case

The results of the modelling of the wet case yielded swelling that was just on the limit of being acceptable when uncompacted pellet filling is used and well within the limits for compacted pellet fillings in compliance with the assumptions made for the design and development work. Since the backfill is modelled with the same properties as the buffer, which corresponds to a density higher than the expected density of the backfill, this case underestimates the swelling.

The conclusion is thus that the design with pellet filling in top of the deposition hole is not acceptable with uncompacted pellet fillings in the wet case.

General comments

The results led to the conclusion that the design with pellet filling in top of the deposition hole is not acceptable and to recommendations to strongly reduce the thickness of the pellet filling between the backfill blocks in the deposition hole and the tunnel blocks if this design would be used.

In the second study the pellet filled part of the deposition hole was replaced by a half block of bentonite in agreement with the present reference design with the same properties as the buffer blocks. Also for this study the two extremes of wet and dry backfill were analysed. The influence of having a bevel or not was also studied.

Dry case

This case was not modelled but analysed analytically with help of old results. The analyse showed that this case could be acceptable if the 10 cm thick pellet filling on the floor was compacted but not if it was only loosely filled. The influence of the bevel is insignificant for this case.

Wet case

The wet case was modelled with finite elements and the results showed that very little swelling and insignificant loss of buffer density on top of the canister occurred also if the pellet filling was uncompacted. Calculations with and without bevel were done and comparisons show that the influence of the bevel on the buffer density is not strong.

The overall conclusion is thus that the dry case is critical and that the reference design with a half block works if the 10 cm thick pellet filling above the deposition hole is compacted.

Sammanfattning

Svällning av bentonitbufferten i deponeringshålen mot återfyllningen och den pelletsfyllda avfasningen kan leda till en densitetsförlust hos bufferten som är oacceptabel. Denna samverkan mellan buffert och återfyllnad har undersökts och modellerats i tidigare projekt. Resultaten visade att det farligaste fallet är en kombination av vattenmättad buffert med fri tillgång till vatten som sväller mot en torr återfyllning och har lett till slutsatser angående designen av främst återfyllningen. Emellertid har designen ändrats och avfasningen i golvet (som inte fanns med i tidigare beräkningar) introducerats för att underlätta installationen av kapseln i deponeringshålen.

För att ytterligare studera buffert/återfyllningens samverkan har följande två studier genomförts:

1. Ny utformning med avfasning, modifierad geometri hos återfyllnadsblocken och pelletsfyllning i toppen på deponeringshålet istället för halvblock.
2. Halvblock i toppen på deponeringshålet som i referensutformningen.

I den första studien har tre beräkningsfall analyserats med finita elementkoden Abaqus. I dessa beräkningar har bufferten modellerats som helt vattenmättad med fri tillgång till vatten. Återfyllningen har modellerad på olika sätt:

- Torra fallet.
  - Torr återfyllning med olika egenskaper hos pelletsfyllningen.
  - Torr återfyllning utan pelletsfyllning i taket.
- Våta fallet.
  - Helt vattenmättad återfyllning med avfasning i golvet.

De komplicerade geometrierna och materialmodellerna och de stora deformationerna som inträffade medförde emellertid avsevärda modelleringsproblem ordsakade av att beräkningarna inte kunde drivas färdigt pga. brist på konvergens. Problemen medförde att förenklingar av modellerna krävdes och att slutsatser ibland måste dras trots ofullständiga beräkningar. Trots dessa problem kunde till slut tillräckligt mycket information tas fram för att dra de slutsatser som presenteras i studien.

Följande slutsatser kunde dras:

Torra fallet

Kompressibiliteten och tjockleken hos pelletsfyllningen i golvet är avgörande egenskaper för buffertens uppsvällning och åtföljande densitetsförlust. Resultaten visar att utformningen med pelletfyllning i toppen av deponeringshålen inte uppfyller kraven varken för packad eller opackad pelletsfyllning.

Inflytandet av egenskaperna hos pelletsfyllningen i taket är inte särskilt stor och beräkningsresultaten tyder på att opackad fyllning fungerar men också att fyllningen behövs och inte kan utelämnas.

Inflytandet av blocken i återfyllnaden i tunneln (i huvudsak egenskaperna hos de horisontella spalterna mellan blocken) är ganska stor särskilt för de fall som är acceptabla. Det är alltså viktigt att öka kunskapen om dessa spalter.

Våta fallet

Modelleringen av det våta fallet gav en svällning som är på gränsen till acceptabel när opackad pelletsfyllning används i överensstämmelse med de gjorda antaganden för design och utvecklingsarbetet och väl inom gränsen när pelletsfyllningen är packad. Eftersom återfyllningen modellerats med samma egenskaper som bufferten, vilket motsvarar en densitet över den förväntade hos återfyllningen, underskattar detta fall svällningen.

Slutsatsen blir därför att utformningen med pelletfyllning i toppen av deponeringshålen även för det våta fallet är oacceptabel om okompakterad pellets läggs i avfasningen.

Allmänna kommentarer

Resultaten leder till slutsatsen att den utformningen med pelletfyllning i toppen av deponeringshålen inte är acceptabel och till rekommendationen att kraftigt minska tjockleken hos pelletsfyllningen mellan återfyllningsblocken i deponeringshålen och tunnel.

I den andra studien ersattes den pelletsfyllda delen av deponeringshålet av ett bentonitblock i överensstämmelse med den nuvarande referensutformningen med samma egenskaper som buffertblocken. Även i denna studie analyserades de två extremerna våt och torr återfyllning. Inverkan av att ha en avfasning eller inte analyserades också.

Torra fallet

Detta fall modellerades inte utan analyserades analytiskt med hjälp av de tidigare resultaten. Analysen visade att detta fall var acceptabelt om den 10 cm tjocka pelletsfyllningen på golvet packades men inte annars. Inverkan av avfasningen blev för detta fall obetydlig.

Våta fallet

Det våta fallet modellerades med finita element och resultaten gav en mycket lite svällning av bufferten och en obetydlig minskning av densiteten vid kapselns lock även om pelletsfyllningen var opackad. Beräkningar med och utan avfasning gjordes och en jämförelse visar att avfasningens inverkan på buffertdensiteten är liten.

Den övergripande slutsatsen är alltså att det torra fallet är dimensionerande och att den referensutformningen med halvblock i deponeringshålets ovandel fungerar om den 10 cm tjocka pelletsfyllningen ovanför deponeringshålet packas.

Contents

1 Introduction

One of the main design requirements of the backfill is to keep the buffer in place and prevent it from swelling upwards so that the buffer will keep its density high enough to fulfil the safety requirements. The acceptance limit of the effect of upwards swelling of the buffer has been set to a decrease in density on top of the canister from the reference density at saturation 2,000 kg/m^3 to 1,950 kg/m^3. This limit has been used because 1,950 kg/m^3 is the lower limit of the density criteria and since the dry density 2,000 kg/m^3 has been used as initial average density in modelling cases. Locally lower density can of course be acceptable and will occur if the average initial dry density before upwards swelling is 1,950 kg/m^3.

For SR-Can both finite element modelling and analytical calculations of this process have been performed (see e.g. Börgesson and Johannesson 2006, Börgesson and Hernelind 2006, Börgesson et al. 2006, Johannesson and Nilsson 2006), but the backfill considered in most of those calculations was an in situ compacted mixture of 30/70 bentonite/crushed rock.

For SR-Site the new backfill (compacted blocks and pellets of Milos backfill) was considered. This backfill behaves very different at dry and wet conditions. Modelling of both cases of this backfill has been done and the results presented in two reports (Johannesson 2008, Börgesson and Hernelind 2009). Special emphasis was given to the swelling under dry backfill conditions in calculations derived for SR-Site in the THM-report (Åkesson et al. 2010).

After the referred calculations were done the design has been modified and a bevel in the rock at the deposition hole was introduced in order to simplify the installation of the canister. Figure 1-1 shows the reference design as described in Figure 3-3 in SKB (2010).

In order to analyse the new design and further develop it the following two studies have been made:

1. New design with bevel, updated backfill block geometries and an alternative with pellet filling in top of the deposition hole.
2. Half block in top of the deposition hole instead of pellet filling as in the reference design.

These items have been studied with finite element simulations and the results of the modelling are reported here.

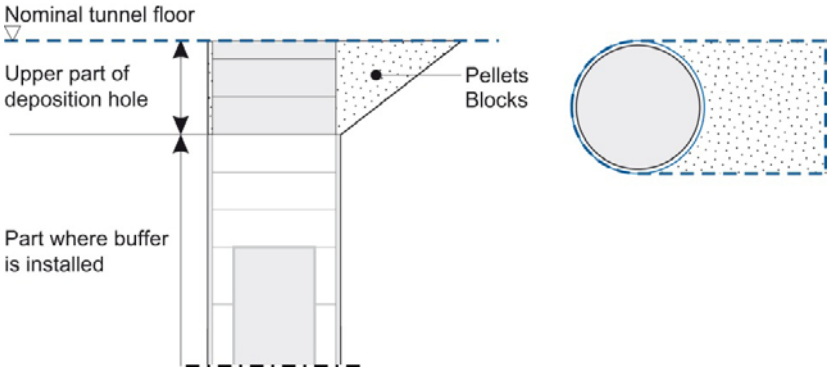

Figure 1-1. *Reference design.*

2 Current knowledge

2.1 General

This chapter summarizes the previous work by the authors regarding the buffer/backfill mechanical interaction when a backfill of piled bentonite blocks and supplementary filling with bentonite pellets are used. The calculations are briefly described. Details are described in the referred documents.

All calculations were made with the simplified assumptions that the buffer is completely water saturated and homogenized from start and that the backfill is either completely water saturated from start (wet case) or completely unaffected by water (dry case). The model of the buffer material refers to the density at saturation 2,000 kg/m^3 and the initial swelling pressure 7.0 MPa. The model is described in Section 5.3.1 and in more detail in Åkesson et al. (2010) and Börgesson et al. (1995).

2.2 Wet case

The finite element calculations of the wet case are described by Börgesson and Hernelind (2009). The finite element model of this case is shown in Figure 2-1. It was a full 3D model of a quarter of a deposition hole and tunnel section with symmetry planes in three of the four vertical boundaries yielding a model of a long tunnel with deposition holes with 6 m distances. There were contact surfaces in all contacts between the rock and the buffer and backfill as well as between the buffer and the canister. The pellet filling at the roof and the walls was included in the model with a thickness of about 0.4 m, but not in the floor.

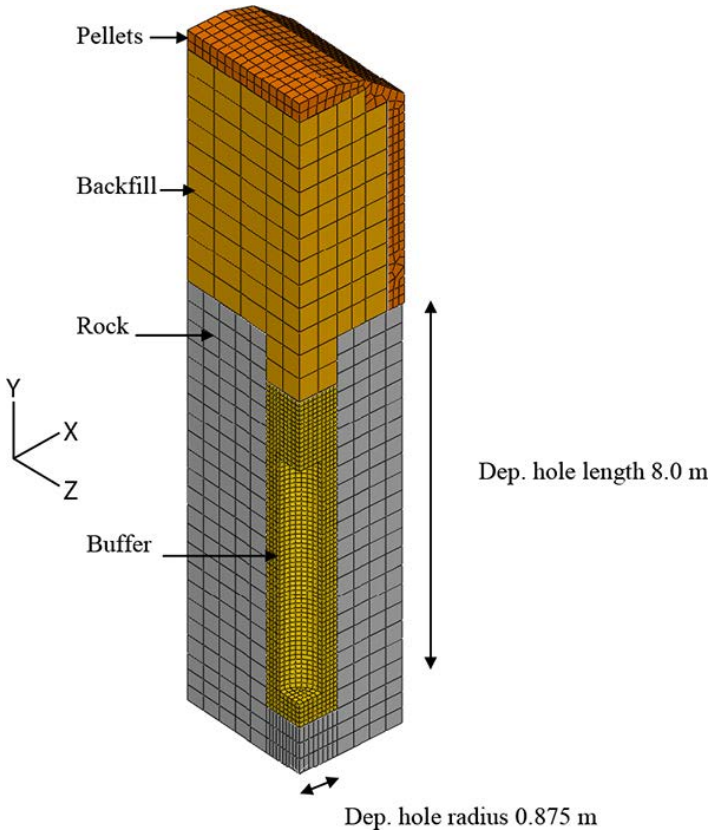

Figure 2-1. *Element mesh for the calculation with wet backfill (the canister is not shown).*

The elastic properties of the backfill material were the following for the base case:

$E_{backfill}$ = 50 MPa

$E_{pellets}$ = 3.24 MPa

ν = 0.3

The friction angle of the all contact surfaces was

ϕ_c = 8.7°

In the base case the swelling pressure of the backfill was

p_0 = 0 MPa (swelling pressure)

Besides the base case, nine different calculations with varying material properties were performed for the wet case. Table 2-1 summarises the results. The table shows the parameters that have been changed compared to the base case, the resulting upwards displacement of the buffer/backfill interface and the heave of the canister after completed swelling.

The influence of the friction angle, the stiffness of the backfill, the stiffness of the pellets filling and the swelling pressure is illustrated by the results. The buffer density on top of the canister is decreased (from 2,000 kg/m^3) to below 1,950 kg/m^3 at an upwards swelling of the buffer/backfill interface of more than about 10 cm. The influence of a swelling pressure in the backfill is especially strong and since we expect a swelling pressure of more than 3 MPa the results show that under normal circumstances the wet case should not be a problem. However, if the swelling pressure is not higher than the design premises 0.1 MPa this case might need some additional investigations. Such low swelling pressure after full water saturation and homogenisation can however only occur under very extreme circumstances such as after huge colloid erosion of backfill material.

Table 2-1. Compilation of modelling results.

Model	Characteristic Deviation from reference model	Displacement of the buffer/ backfill interface (mm)	Canister heave (mm)
Baclo3b	Reference model	102.9	5.5
Baclo3b1	ϕ_c = 4.4°	116.1	8.0
Baclo3b2	ϕ_c = 17.0°	94.3	3.5
Baclo3b3	ϕ_c = 0°	153.9	50.0
Baclo3b4	$E_{pellets}$ = $E_{backfill}$ = 50 MPa	94.4	5.0
Baclo3b5	$E_{backfill}$ = 25 MPa	145.7	7.0
Baclo3b6	$E_{backfill}$ = 100 MPa	74.1	3.7
Baclo3b7d	p_0 = 3 MPa, $E_{pellets}$ = 50 MPa	23.9	0.8
Baclo3b7e	p_0 = 1 MPa, $E_{pellets}$ = 50 MPa	44.4	1.7
Baclo3b8	p_0 = 3 MPa, $E_{pellets}$ = 50 MPa, ϕ_c = 0°	58.4	17.0

2.3 Dry case

The modelling of the dry case is described in the THM report (Åkesson et al. 2010). The finite element model was almost identical to the model of the wet case with the exception that the pellets filling on the floor was included and that each separate block was modelled with 4 mm slots between the blocks. Figure 2-2 shows the model.

The pellets filled slot at the roof was 0.3 m at the crown but a second model with the upper backfill block row replaced with pellets filling was also used yielding 0.55 m slot. The slot between the rock wall and the blocks was 0.29 m wide and the pellets filling in the floor was 0.3 m thick with exception of above the upper backfill block in the deposition hole where the pellets filling was only 0.08 m. Two block types were used; one with the dimensions 0.667 × 0.7 × 0.51 m^3 and one with the dimensions 0.6 × 0.7 × 0.25 m^3. There was a slot of 4 mm between all blocks for both horizontal and

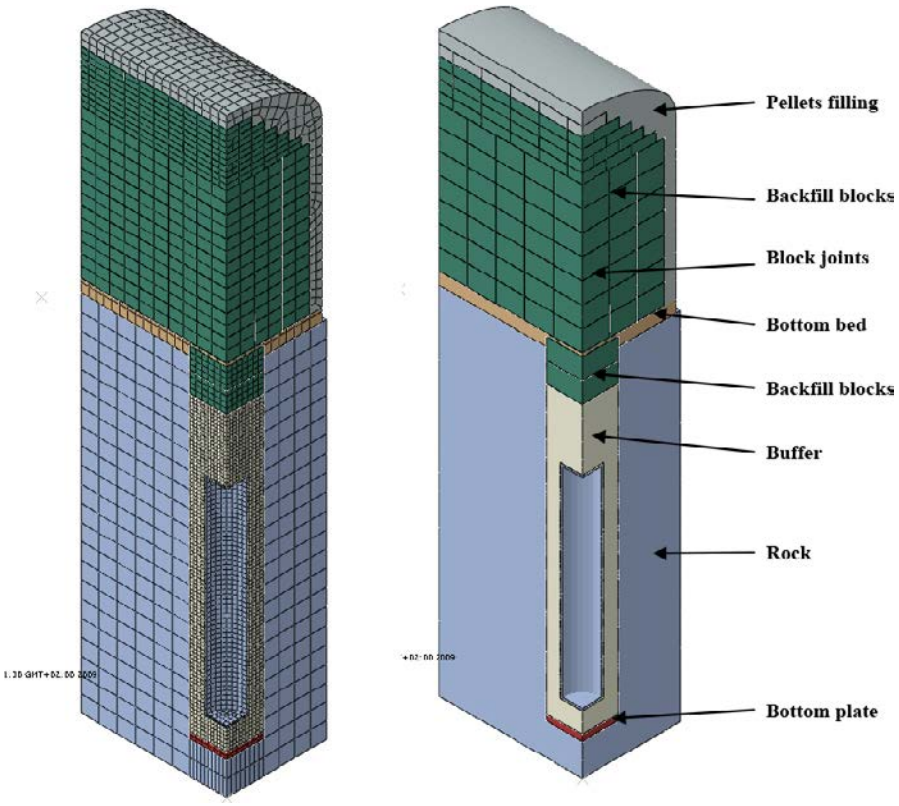

Figure 2-2. *3D element model of a deposition tunnel section with a deposition hole. The left picture shows the element mesh while the right picture shows the different property domains and all the backfill blocks separated by slots.*

vertical slots. This slot simulates the irregularities of the backfill blocks that after piling will result in imperfect contact areas. Altogether this geometry yields a degree of block filling of about 76% (volume block divided to actual tunnel volume).

There were thus three different parts included in the dry backfill, namely the blocks, the joints between the slots and the pellets filling.

The backfill blocks will according to the reference design in the production line report be compacted with a water content of 17% to a dry density of 1,700 kg/m^3. Unfortunately no measurements of the elastic properties of the reference material Milos backfill have been done but measurements on similar materials have yielded similar results (see Section 5.3.2). The blocks are very stiff compared to the pellets filling and the joints so the results are rather insensitive to the elastic properties of the blocks.

The backfill blocks were modelled as a linear elastic material with the following properties:

E = 245 MPa

v = 0.17

where v = Poisson´s ratio and E = modulus of elasticity.

The initial average stress was p_0 = 0 MPa.

The compressibility of different pellets fillings have been tested and reported by Johannesson (2008). They were modelled as linear elastic. There were two types of pellets filling with different properties. The pellets filling in the walls and in the roof was a loose filling with the following parameters:

E = 3.9 MPa

v = 0.3

The compacted pellets filling of the bottom bed in the floor is stiffer and was given the following parameters:

$E = 10$ MPa

$\nu = 0.3$

Since the bottom bed on which the blocks rest cannot be made as a completely plane or horizontal surface the backfill blocks will be placed slightly uneven in relation to each other. This means that there will be joints that are not even due to slightly inclined blocks that also have slightly different heights. The properties of these joints between the blocks are not known but they will have compression and friction properties that deviate significantly from the properties of the blocks.

The joints were assumed to have the following properties (both horizontal and vertical):

- Average joint thickness: 4 mm.
- Compression properties: The 4 mm joints are closed at an external pressure of 10 MPa.
- Friction angle $\phi = 20^{\circ}$.

See also Section 5.3.2.

Three calculations were made with variation of the buffer density and the width of the pellets filled slot at the roof. Table 2-2 shows a compilation of the results. Figure 2-3 shows an example of the results from Model 1.

The results show that there was a loss in density of the buffer above the canister but the resulting lowest density at water saturation at the canister/buffer contact at the initial density 2,000 kg/m^3 was 1,960 kg/m^3, which is acceptable. If the initial density is only 1,950 kg/m^3 the corresponding density is 1,920 kg/m^3, but the swelling pressure is 2.1 MPa so this result should also be acceptable as an extreme case although the density is lower than the density criteria (1,950 kg/m^3). The results also show that there may locally, in some backfill blocks on the floor, be Mises' stresses that are higher than the compressive strength (2–4 MPa) and thus may cause local crushing of the blocks. This is not expected to yield any problems.

The effect of increasing the aperture of the pellets filled slot at the roof from 30 cm to 55 cm was not very strong, which was caused by the masonry of the smaller blocks (overlapping in contrast to the larger blocks). If no overlapping of the blocks close to the roof the total upwards swelling would probably be higher!

Another conclusion was that both block types should be piled with overlapping, which probably would reduce the upwards swelling!

Table 2-2. Summary of results.

Variable	Model 1	Model 2	Model 3
Density at saturation	2,000 kg/m^3	2,000 kg/m^3	1,950 kg/m^3
Pellets filled slot	30 cm	55 cm	55 cm
Max buffer upwards swelling	96 mm	102 mm	68 mm
Canister heave	4.8 mm	5.0 mm	3.2 mm
Buffer density at top of canister	1,960 kg/m^3	1,960 kg/m^3	1,920 kg/m^3
Average axial swelling pressure at top of canister	3.8 MPa	3.6 MPa	2.1 MPa

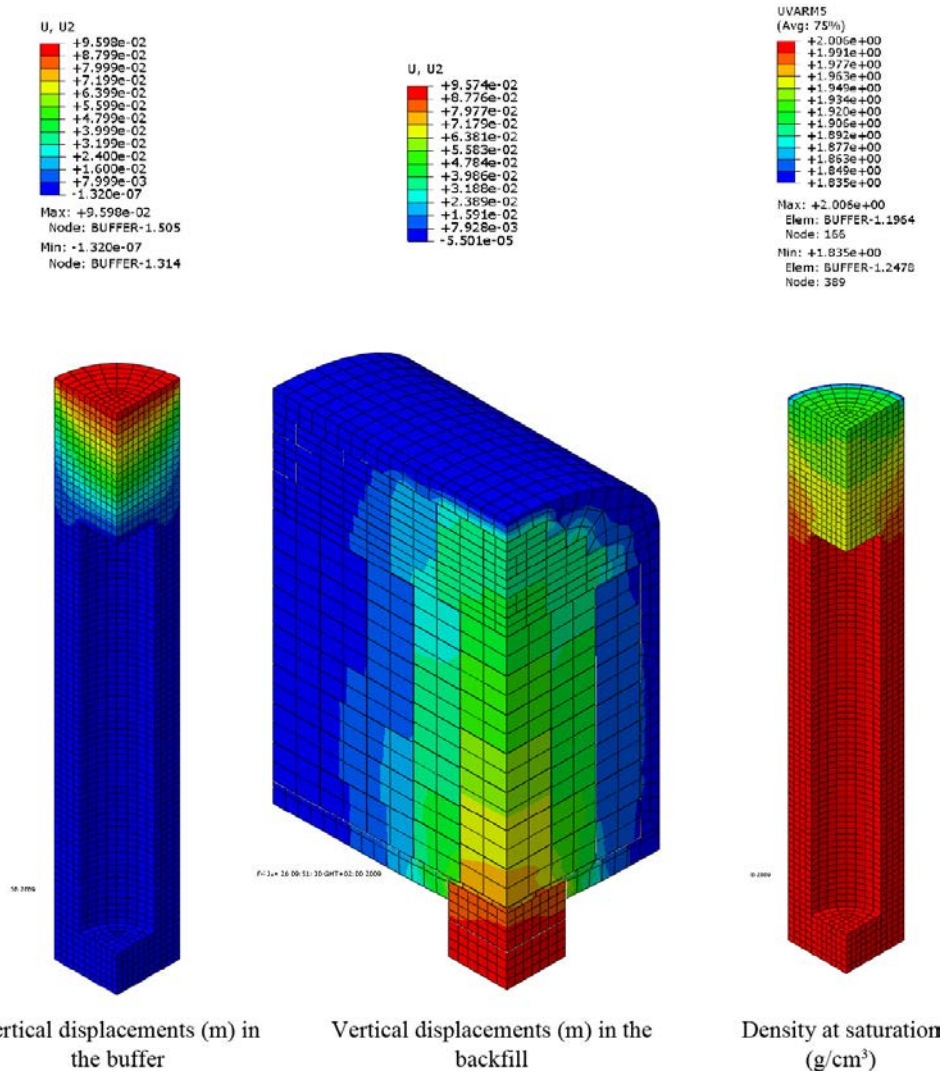

Figure 2-3. *Final state of the buffer and backfill after completed swelling. The vertical displacements and the density are shown for model 1 with 30 cm pellets filled slot at the roof and the buffer density 2000 kg/m^3.*

3 Problem description

The objective of the new study is to update the finite element model used in Börgesson and Hernelind (2009) to better correspond to the present design by including the bevel in the deposition hole, the bottom bed of bentonite pellets and the proposed masonry of overlapping backfill blocks and to study.

- The influence of the design and properties of the bottom bed.
- The influence of the pellets filling at the roof and in the upper part of the deposition hole.
- The influence of the bevel and the properties of the bevel filling.

The proposed geometry was given by SKB and has been directly imported into the element mesh in Abaqus. The geometry is shown in Figure 3-1.

This geometry differs from the reference design since the upper half block is replaced by pellets. One of the purposes of the presented calculations was to investigate if this design could be used. The geometry in Figure 3-1 corresponds to the nominal tunnel geometry, which yields the highest average dry density in the interval 1,458–1,535 kg/m^3 according to the production line report (SKB 2010). The influence of lower average dry density due to larger rock cross sections has been handled in the analyses.

Previous investigations and calculations have shown that the dry case is more critical than the wet case mainly due to the swelling pressure of the backfill that strongly limits the swelling of the buffer in the wet case. This swelling pressure is not present in the dry case.

The dry case is rather unrealistic and must be considered a pessimistic upper limit of swelling. The main principle is that the buffer is kept water saturated and may swell with unlimited access to water while the backfill is dry and completely unaffected by water. The problem is to set the boundary between them since the upper two blocks in the deposition hole belongs by definition to the backfill. There are two possibilities, either to keep those blocks dry or to make them belong to the buffer and make them wet and swelling. The former alternative was chosen for all modelling cases since the blocks belong to the backfill and the latter alternative would yield a much more complicated calculation due to the swelling of these bentonite blocks into the bevel.

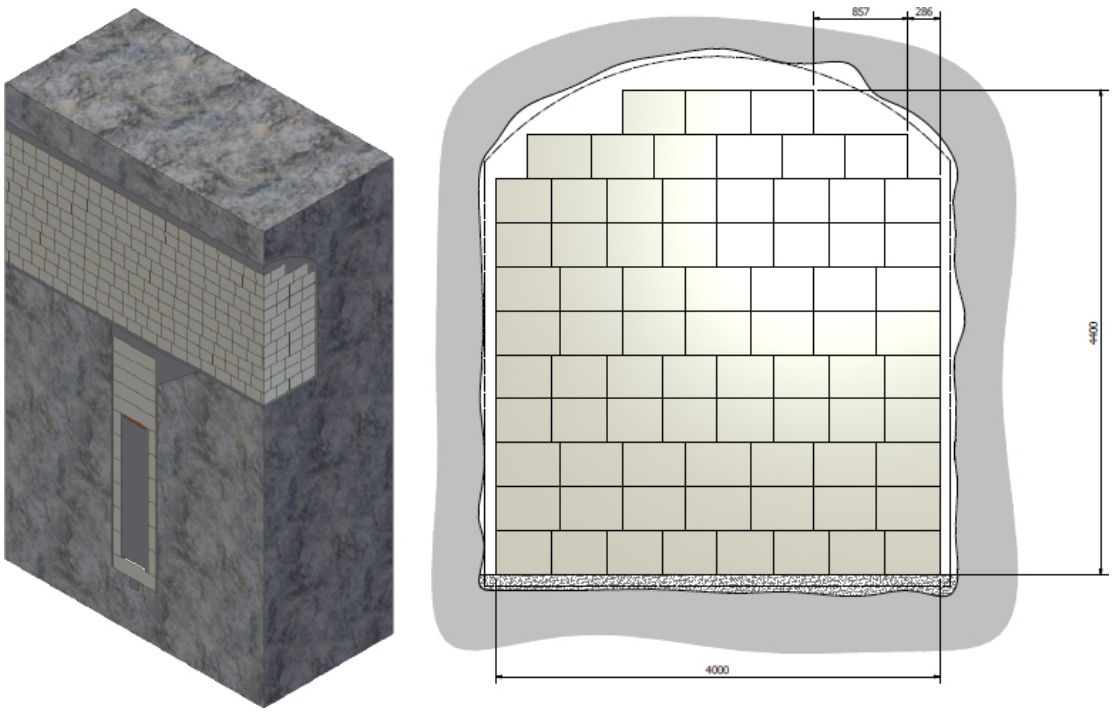

Figure 3-1. *Geometry of the backfill imported to Abaqus.*

The dry case thus means that the bevel is insignificantly affected in the calculation since the two upper dry bentonite blocks are merely just displaced vertically. However, for the wet case the bevel is strongly affected and compressed by the swelling of the upper and sideways backfill blocks.

In order to further study the buffer / backfill interaction the following two studies have been made:

1. Bevel, updated backfill block geometries and pellet filling in top of the deposition hole instead of half-block.
2. Half-block in top of the deposition hole as in the reference design.

In the first study (1A and 1B) three types of calculations have been performed with the finite element code Abaqus. In these calculations the buffer has been modelled as completely water saturated with free access to water. The backfill has been modelled in different ways:

- Dry case.
  - Dry backfill with different properties of the pellet fillings.
  - Dry backfill without pellet filling at the roof.
- Wet case.
  - Completely water saturated backfill with bevel.

These calculations are described in Chapters 5 and 6.

In the second study (2A and 2B) pellet filled part of the deposition hole was replaced by a bentonite block with the same properties as the buffer blocks. Also for this study the two extremes of wet and dry backfill were analysed. The influence of having a bevel or not was also studied.

These calculations are described in Chapter 7.

In Table 3-1 the calculations are summarised.

Table 3-1. Reported calculations.

Modelled case	Variant	Pellet properties	Number of calculations	Remarks
1A. Pellets instead of half-block in top of deposition hole – dry case	1A1. With bevel	Very stiff pellets in the floor and at the roof	1	
		No pellets at the roof	1	
	1A2. Without bevel	Different stiffness of the pellets in the floor and at the roof	4	
1B. Pellets instead of half-block in top of deposition hole – wet case	1B1. With bevel	Different stiffness of the pellets in the bevel	2	
2A. Half-block in top of deposition hole – dry case	2A1. With bevel	Different stiffness of the pellet filling	2	Analytical consideration
	2A2. Without bevel	Low stiffness	1	Analytical consideration
2B. Half-block in top of deposition hole – wet case	2B1. With bevel	Low stiffness	1	
	2B2. Without bevel	Low stiffness	1	

4 Finite element code

4.1 General

The finite element code Abaqus was used for the calculations. Abaqus contains a capability of modelling a large range of processes in many different materials as well as complicated three-dimensional geometry.

The code includes special material models for rock and soil and ability to model geological formations with infinite boundaries and in situ stresses by e.g. the own weight of the medium. It also includes capability to make substructures with completely different finite element meshes and mesh density without connecting all nodes. Detailed information of the available models, application of the code and the theoretical background is given in the Abaqus manuals.

4.2 Hydro-mechanical analyses in Abaqus

The hydro-mechanical model consists of porous medium and wetting fluid and is based on equilibrium, constitutive equations, energy balance and mass conservation using the effective stress theory.

Equilibrium

Equilibrium is expressed by writing the principle of virtual work for the volume under consideration in its current configuration at time t:

$$\int_V \boldsymbol{\sigma} : \delta\boldsymbol{\varepsilon}\, dV = \int_S \mathbf{t} \cdot \delta\mathbf{v}\, dS + \int_V \hat{\mathbf{f}} \cdot \delta\mathbf{v}\, dV \tag{4-1}$$

where $\delta\mathbf{v}$ is a virtual velocity field, $\delta\boldsymbol{\varepsilon} \overset{def}{=} sym\left(\partial\delta\mathbf{v}/\partial\mathbf{x}\right)$ is the virtual rate of deformation, $\boldsymbol{\sigma}$ is the true (Cauchy) stress, $\mathbf{t}$ are the surface tractions per unit area, and $\hat{\mathbf{f}}$ are body forces per unit volume. For our system, $\hat{\mathbf{f}}$ will often include the weight of the wetting liquid,

$$\mathbf{f}_w = S_r n \rho_w \mathbf{g} \tag{4-2}$$

where S_r is the degree of saturation, n the porosity, ρ_w the density of the wetting liquid and $\mathbf{g}$ is the gravitational acceleration, which we assume to be constant and in a constant direction. For simplicity we consider this loading explicitly so that any other gravitational term in $\hat{\mathbf{f}}$ is only associated with the weight of the dry porous medium. Thus, we write the virtual work equation as

$$\int_V \boldsymbol{\sigma} : \delta\boldsymbol{\varepsilon} dV = \int_S \mathbf{t} \cdot \delta\mathbf{v} dS + \int_V \mathbf{f} \cdot \delta\mathbf{v} dV + \int_V S_r n \rho_w \mathbf{g} \cdot \delta\mathbf{v} dV \tag{4-3}$$

where $\mathbf{f}$ are all body forces except the weight of the wetting liquid.

The simplified equation used in Abaqus for the effective stress $\overline{\boldsymbol{\sigma}}^*$ is:

$$\overline{\boldsymbol{\sigma}}^* = \boldsymbol{\sigma} + \chi\, u_w \mathbf{I} \tag{4-4}$$

where $\boldsymbol{\sigma}$ is the total stress, u_w is the pore water pressure, χ is a function of the degree of saturation (usual assumption $\chi = S_r$), and $\mathbf{I}$ the unitary matrix.

Energy balance

The conservation of energy implied by the first law of thermodynamics states that the time rate of change of kinetic energy and internal energy for a fixed body of material is equal to the sum of the rate of work done by the surface and body forces. This can be expressed as:

$$\frac{\mathrm{d}}{\mathrm{dt}} \int_V \left(\tfrac{1}{2}\rho\mathbf{v}\cdot\mathbf{v} + \rho U\right) \mathrm{dV} = \int_s \mathbf{v}\cdot\mathbf{t}\,\mathrm{dS} + \int_V \mathbf{f}\cdot\mathbf{v}\,\mathrm{dV} \tag{4-5}$$

where

ρ is the current bulk density,

v is the velocity field vector,

U is the internal energy per unit mass,

t is the surface traction vector,

f is the body force vector.

Constitutive equations

The constitutive equation for the solid is expressed as:

$$d\boldsymbol{\tau}^{c} = \mathbf{H} : d\boldsymbol{\varepsilon} + \mathbf{c} \tag{4-6}$$

where $d\boldsymbol{\tau}^{c}$ is the stress increment, **H** the material stiffness, $d\boldsymbol{\varepsilon}$ the strain increment and **c** is any strain independent contribution (e.g. thermal expansion). **H** and **g** are defined in terms of the current state, direction for straining, etc., and of the kinematic assumptions used to form the generalised strains.

The constitutive equation for the liquid (static) in the porous medium is expressed as:

$$\frac{\rho_{\mathrm{w}}}{\rho_{\mathrm{w}}^{0}} \approx 1 + \frac{\mathrm{u}_{\mathrm{w}}}{\mathrm{K}_{\mathrm{w}}} - \varepsilon_{\mathrm{w}}^{\mathrm{th}} \tag{4-7}$$

where ρ_w is the density of the liquid, ρ_{w}^{0} is its density in the reference configuration, $K_w(T)$ is the liquid's bulk modulus, and

$$\varepsilon_{w}^{th} = 3\alpha_{w}(T - T_{w}^{0}) - 3\alpha_{w|T^{I}}(T^{I} - T_{w}^{0}) \tag{4-8}$$

is the volumetric expansion of the liquid caused by temperature change. Here $\alpha_w(T)$ is the liquid's thermal expansion coefficient, T is the current temperature, T^{I} is the initial temperature at this point in the medium, and T_{w}^{0} is the reference temperature for the thermal expansion. Both $\mathrm{u_w/K_w}$ and $\varepsilon_{\mathrm{w}}^{\mathrm{th}}$ are assumed to be small.

Mass conservation

The mass continuity equation for the fluid combined with the divergence theorem implies the point wise equation:

$$\frac{1}{J}\frac{d}{dt}\left(J\rho_{\mathrm{w}} S_r n\right) + \frac{\partial}{\partial \mathbf{x}} \cdot \left(\rho_{\mathrm{w}} S_r n \mathbf{v}_{\mathrm{w}}\right) = 0 \tag{4-9}$$

where J is the determinant of the Jacobian matrix of the skeleton motion and **x** is position. The constitutive behaviour for pore fluid is governed by Darcy's law, which is generally applicable to low fluid velocities. Darcy's law states that, under uniform conditions, the volumetric flow rate of the wetting liquid through a unit area of the medium, $S_r n\mathbf{v}_w$, is proportional to the negative of the gradient of the piezometric head:

$$S_r n \mathbf{v}_{\mathrm{w}} = -\hat{\mathbf{k}} \frac{\partial \phi}{\partial \mathbf{x}} \tag{4-10}$$

where $\hat{\mathbf{k}}$ is the permeability of the medium and ϕ is the piezometric head, defined as:

$$\phi \overset{def}{=} \mathrm{z} + \frac{\mathrm{u}_{\mathrm{w}}}{\mathrm{g}\rho_{\mathrm{w}}} \tag{4-11}$$

where z is the elevation above some datum level and g is the magnitude of the gravitational acceleration, which acts in the direction opposite to z. $\hat{\mathbf{k}}$ can be anisotropic and is a function of the saturation and void ratio of the material. $\hat{\mathbf{k}}$ has units of velocity (length/time). [Some authors refer to $\hat{\mathbf{k}}$ as the hydraulic conductivity and define the permeability as:

$$\hat{\mathbf{K}} = \frac{v}{g}\hat{\mathbf{k}} \tag{4-12}$$

where v is the kinematic viscosity of the fluid.]

We assume that g is constant in magnitude and direction, so

$$\frac{\partial \phi}{\partial \mathbf{x}} = \frac{1}{\mathrm{g}\rho_{\mathrm{w}}}\left(\frac{\partial \mathrm{u}_{\mathrm{w}}}{\partial \mathbf{x}} - \rho_{w}\mathbf{g}\right) \tag{4-13}$$

4.3 Handling of buffer and backfill processes

Overviews of how Abaqus handles the THM-processes for buffer and backfill materials are given in other SKB reports (see e.g. Åkesson et al. 2010). Constitutive relations, choice of parameter values and calculation strategies are described.

5 Upwards swelling against dry tunnel – case 1A

5.1 General

Case 1A (see Table 3-1) refers to the case with pellets instead of half-block in top of deposition hole and dry backfill. For this case the two issues of the influence of the bottom bed and the pellet filling at the roof were studied with (initially) the same finite element model. However, the calculations have involved huge convergence problems and could finally only be made after simplifications of the element mesh.

5.2 Finite element mesh

A 3D element model of a section of the tunnel with backfill and a deposition hole with buffer, canister and the bottom plate is used. The geometry was taken from the SKB model shown in Figure 3-1. Figure 5-1 shows the element mesh.

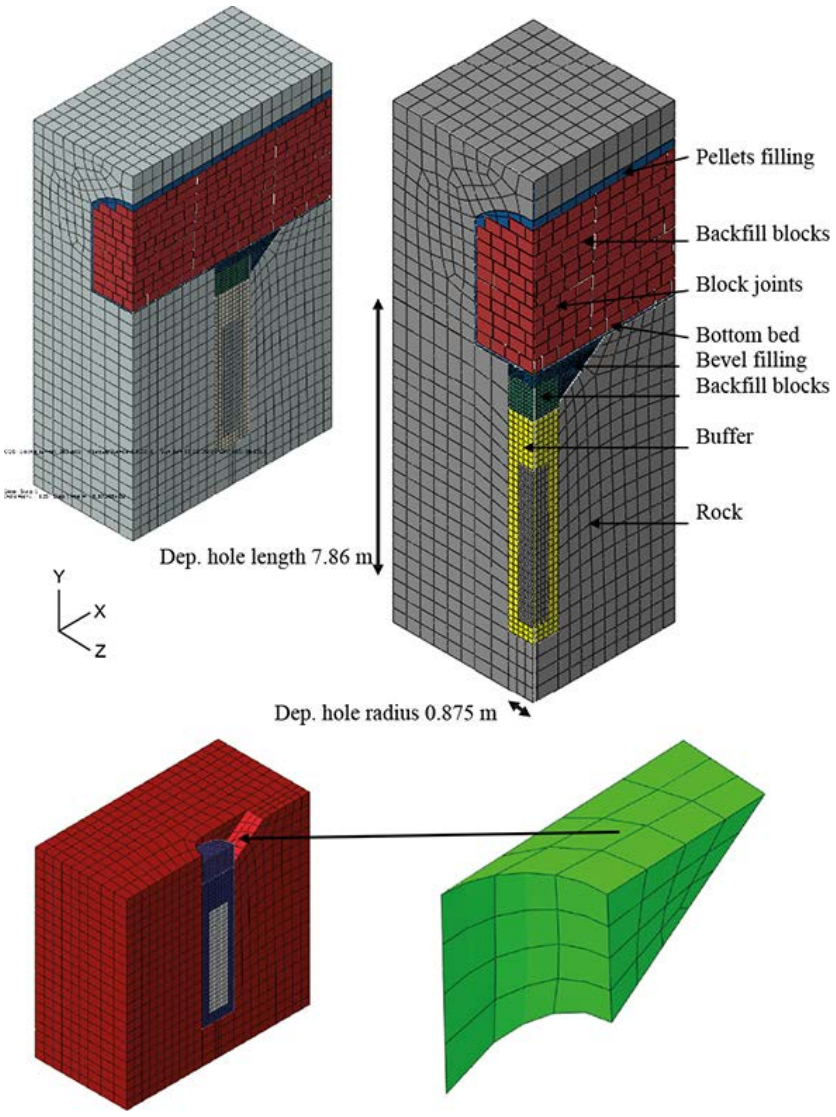

Figure 5-1. *Upper: 3D element model of a deposition tunnel section with a deposition hole. The left picture shows the entire element mesh while the right picture shows half the model with the different property domains. Lower: Illustration of the geometry of the bevel (not the mesh).*

The model simulates a long tunnel with deposition holes at every 6th meter but is simplified to half a deposition hole section by using symmetry planes in three of the four vertical boundaries. There are contact surfaces in all contacts between the rock and the buffer and backfill as well as between the buffer and the canister.

The pellets filled slot at the roof is 0.3 m at the crown. The slot between the rock wall and the blocks is 0.1 m wide and the pellets filling in the floor (bottom bed) is also 0.1 m. Above the upper backfill block in the deposition hole the pellets filling is 0.36 m thick in addition to the 0.1 m of the bottom bed. This differs from the current reference case where it is 0.25 m in addition to the bottom bed. The dimensions of the blocks are 0.571x0.5x0.40 m^3 and in the model cut at the symmetry boundaries to fit. The geometry supplied by SKB contains no slot between the blocks. The slot is thus instead modelled by the material definition for the contact surfaces simulating the 4 mm slot. This slot simulates the irregularities of the backfill blocks that after piling will result in imperfect contact areas.

The bevel in the deposition hole is filled with pellets with the same properties as the other pellet filled parts. The bevel is also illustrated in Figure 5-1, but the figure only shows the geometry. The real mesh of the bevel is much more refined.

The element mesh has been varied slightly during the attempts to make the calculations converge but all meshes are very similar to the one shown.

The size of the model is approximately 40,000 elements, 73,000 nodes and 350,000 variables. Some of the calculations were very time consuming with up to about 2,000 hours CPU time corresponding to 500 hours wall clock time.

All elements are linear except for the rock that has quadratic elements. Most simulations are done with large strains and large displacements.

5.3 Material properties

5.3.1 Buffer material

The buffer material model is identical to the model used for studying the behaviour of water saturated buffer material (see e.g. Åkesson et al. 2010 and Börgesson et al. 1995). The bentonite is modelled as completely water saturated and homogenised from start with the average void ratio 0.77 corresponding to the density at full water saturation 2,000 kg/m^3 in the entire buffer. The motivation for assuming full water saturation and homogenisation is manifold:

- The mechanical models of unsaturated bentonite are very complicated and not sufficiently good for modelling the strong swelling that may take place.
- The models for water saturated bentonite are much more reliable and well documented.
- The stress path and time schedule will differ if saturated instead of unsaturated bentonite is modelled but the final state will be very similar.

Porous Elasticity combined with *Drucker Prager Plasticity* has been used for the swelling/ consolidation mechanisms, while *Darcy's law* is applied for the water flux and the *Effective Stress Theory* is applied for the interaction pore water and structure.

Mechanical properties

For detailed descriptions see Åkesson et al. (2010) and Börgesson et al. (1995).

The *Porous Elastic Model* implies a logarithmic relation between the void ratio e and the average effective stress p according to Equation 5-1.

$$\Delta e = \kappa/(1 + e_0)\Delta \ln p \qquad (5\text{-}1)$$

where κ = porous bulk modulus, e_0 = initial void ratio

Poisson's ratio v is also required.

Drucker Prager Plasticity model contains the following parameters:

β = friction angle in the p-q plane

d = cohesion in the p-q plane

ψ = dilation angle

$q = f(\varepsilon^d_{pl})$ = yield function

The yield function is the relation between Mises' stress q and the plastic deviatoric strain e^d_p at a specified stress path. The dilation angle determines the volume change during shear.

The following data has been derived and used for the *Porous Elastic* model (valid for e<1.5):

$\kappa = 0.21$

$\nu = 0.4$

The following data has been derived for the *Drucker Prager Plasticity* model

$\beta = 17°$

d = 100 kPa

$\psi = 2°$

Yield function: see Table 5-1, where the plastic strain ε_{pl} is given as a function of the Mises stress q.

In some calculations the data for the *Drucker Prager Plasticity* model has been varied in order to study the influence of the friction angle, the cohesion and the dilation.

Hydraulic properties

The hydraulic conductivity is a function of the void ratio as shown in Table 5-2.

Table 5-1. Yield function.

q **(kPa)**	ε_{pl}
113	0
138	0.005
163	0.02
188	0.04
213	0.1

Table 5-2. Relation between hydraulic conductivity and void ratio (Börgesson et al. 1995).

e	***K*** **(m/s)**
0.45	$1.0 \cdot 10^{-14}$
0.70	$8.0 \cdot 10^{-14}$
1.00	$4.0 \cdot 10^{-13}$
1.5	$2.0 \cdot 10^{-12}$
2.00	$1.0 \cdot 10^{-11}$
3.00	$2.0 \cdot 10^{-11}$
5.00	$7.0 \cdot 10^{-11}$
10.00	$3.0 \cdot 10^{-10}$
20.00	$1.5 \cdot 10^{-9}$

Interaction pore water and structure

The effective stress theory states that the effective stress (the total stress minus the pore pressure) determines all the mechanical properties. It is modelled by separating the function of the pore water and the function of the particles. The density ρ_w and bulk modulus K_w of the pore water as well as the density ρ_S and the bulk modulus of the solid particles K_S are required parameters. The following standard values for Na-bentonite are used in the model:

Pore water

$\rho_w = 1{,}000$ kg/m^3 (density of water)

$K_w = 2.1 \cdot 10^6$ kPa (bulk modulus of water)

Particles

$\rho_S = 2{,}780$ kg/m^3 (density of solids) (Karnland et al. 2006)

$K_S = 2.1 \cdot 10^8$ kPa (bulk modulus of solids)

Initial conditions

All calculations were done with the same initial conditions of the buffer. The buffer is completely water saturated and is assumed to have an average density at saturation of $\rho_m = 2{,}000$ kg/m^3 or the void ratio $e = 0.77$ corresponding to the average density in the deposition hole. The pore pressure is set to $u = -7$ MPa in order to correspond to the effective average stress $p = 7$ MPa that yields zero total average stress. The initial conditions of the buffer are thus:

$u_0 = -7$ MPa

$p_0 = 7$ MPa

$e_0 = 0.77$

5.3.2 Backfill

There are three different parts included in the dry backfill, namely the blocks, the joints between the slots and the pellets filling.

Block section

The backfill blocks will according to the reference design in the production line report be compacted with a water content of 17% to a dry density of 1,700 kg/m^3. Measurements of the elastic properties of potential backfill materials (e.g. Asha and IBECO-RWC-BF (Johannesson 2008)) have yielded fairly equal results. The blocks are very stiff compared to the pellets filling and the joints so the results are rather insensitive to the elastic properties of the blocks.

The backfill blocks are modelled as a linear elastic material with the following properties:

$E = 245$ MPa

$\nu = 0.17$

Initial average stress $p_0 = 0$ MPa

Pellet section

The parts filled with pellets are modelled with linear elasticity and Drucker Prager plasticity. The properties of the pellets filling have been varied in order to analyse the influence of the stiffness. There are two types of pellets filling which may have different properties but the plastic behaviour is the same and modelled with Drucker-Prager plasticity. For detailed descriptions see Åkesson et al. (2010) and Börgesson et al. (1995).

Table 5-3. Yield function.

q (kPa)	ε_{pl}
100	0

Drucker Prager plasticity

$\beta = 55°$ (corresponds to a Mohr-Coulomb friction angle of $\phi = 30°$)

$d = 52$ kPa

$\psi = 0°$

Walls and roof

Three different E-modules of the pellets filling at the roof and walls have been used:

$E_1 = 3.9$ MPa (base case)

$E_2 = 10$ MPa (stiff)

$E_3 = 20$ MPa (stiffer)

$v = 0.3$

Initial average stress $p_0 = 0$ MPa

The base case corresponds to the stiffness that the pellet filling will have when it has not been compacted.

Bottom bed and bevel

The pellets filling in the floor and in the bevel has also been varied and given the same parameters but is in some case different from the pellet filling in the roof and walls:

$E_1 = 3.9$ MPa (base case)

$E_2 = 10$ MPa (stiff)

$E_3 = 20$ MPa (stiffer)

$v = 0.3$

Initial average stress $p_0 = 0$ MPa

The compressibility of different pellets fillings have been tested and reported by Johannesson (2008). The E-modules used are evaluated from those measurements for an increase in stress from 0 to 1 MPa for the pellets in the roof and walls and from 0 to 3 MPa for compacted pellets filling (stiff).

The base case E_1 corresponds to uncompacted filling, E_2 corresponds to compacted filling and E_3 is a very stiff filling that is used for modelling purpose in order to facilitate convergence.

Joints between blocks

Since the bottom bed on which the blocks rest cannot be made as a completely plane or horizontal surface the backfill blocks will be placed slightly uneven in relation to each other. This means that there will be joints that are not even due to slightly inclined blocks that also have slightly different heights. The properties of these joints between the blocks are not known but they will have compression and friction properties that deviate significantly from the properties of the blocks.

The following properties have been applied to the joints (both horizontal and vertical):

- Average joint thickness: 4 mm (fictive).
- Compression properties: The joints are closed at an external pressure of 10 MPa.
- Friction angle $\phi = 20°$.

Figure 5-2 shows the stress-compression relation that has been used for the joints.

The joint is a contact surface property where the contact pressure is defined versus the normal vertical displacement.

5.3.3 Canister

The canister is modelled as very stiff with the following fictive elastic parameters:

$E = 2.1 \cdot 10^6$ MPa

$\nu = 0.3$

5.3.4 Rock

The rock is modelled as an elastic material with high stiffness.

$E = 1.85 \cdot 10^8$ kPa

$\nu = 0.3$

5.3.5 Contact surfaces

The contact between *the buffer and the rock* and the *pellets filling and the rock* has not been tied in order to allow slip. Instead interface properties with a specified friction have been applied between the different materials. The friction has been modelled with Mohr Coulomb's parameter friction angle ϕ and without cohesion c.

The following basic value has been used for the contact rock/buffer:

$\phi = 8.69°$

c = 0

This friction angle corresponds to the friction angle of the buffer material $\beta = 17°$ in the Drucker Prager model, which means that the rock surface is considered rough.

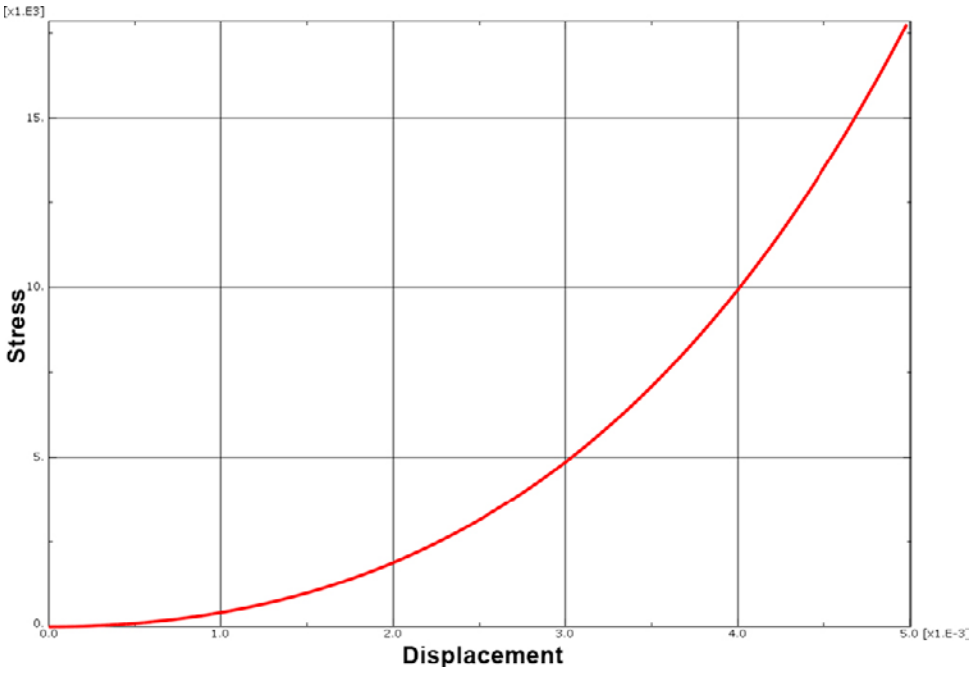

Figure 5-2. *Mechanical model of the joints between blocks. The displacement or compression (m) of the joint is plotted as a function of the total stress (kPa) perpendicular to the joint. After 4 mm compression the 4 mm joint is closed.*

The following values have been used for the contact pellets/rock and the contact pellets/backfill blocks:

$\phi = 30°$

$c = 0$

This friction angle corresponds to the friction angle of the pellets filling b = 55° in the Drucker Prager model, which means that the contact surfaces are considered rough. See Appendix F in Glamheden et al. (2010).

The contact surfaces are made not to withstand tensile stress, which means that the contact may be lost and a gap formed between the surfaces.

Another property of the contact surface is the so called "slip tolerance", which describes the required slip to reach full friction. This parameter has been set to 1 mm. Below 1 mm slip the friction is proportional to the slip.

5.4 Boundary conditions

The following boundary conditions are applied (see also Figure 5-1):

Mechanical

The vertical boundary planes are symmetry planes and free to move parallel with the plane and fixed perpendicular to the plane.

The horizontal boundaries are fixed.

Hydraulic

Only the buffer is modelled hydraulically with pore pressure elements. The buffer boundaries to the rock have constant water pressure (u = 0 MPa), the boundaries to the canister are no flow boundaries and the vertical symmetry plane is a no flow boundary.

5.5 Calculation sequence

The calculations are coupled hydro-mechanical calculations. The pore water pressure in the hydraulic boundary of the buffer is ramped on from –7 MPa to 0 MPa during 1,000 seconds. Then the actual consolidation calculation is run until complete pore water pressure equilibrium with pore pressure 0 MPa is reached in the entire buffer. The displacements were finished and the pore pressure equalized in less than 30 years.

The calculations included a technique for facilitating the convergence conditions by introducing damping forces. This implies that the simulated time until pore pressure equilibrium will be extended and that the time until the swelling is completed thus is not physical.

5.6 Results

The history plots of displacements are given for different points in the centre line of the deposition hole. Figure 5-3 shows the location of those points.

Contour plots of stresses, displacements, void ratio and wet density (density at saturation) at the end of the calculations are shown. All figures show the deformed mesh with no magnification.

Wet density ρ_m is calculated from the void ratio e and the density of solids ρ_s (= 2,780 kg/m^3) according to Equation 5-2.

$$\rho_m = (\rho_s + e)/(e + 1) \qquad (5\text{-}2)$$

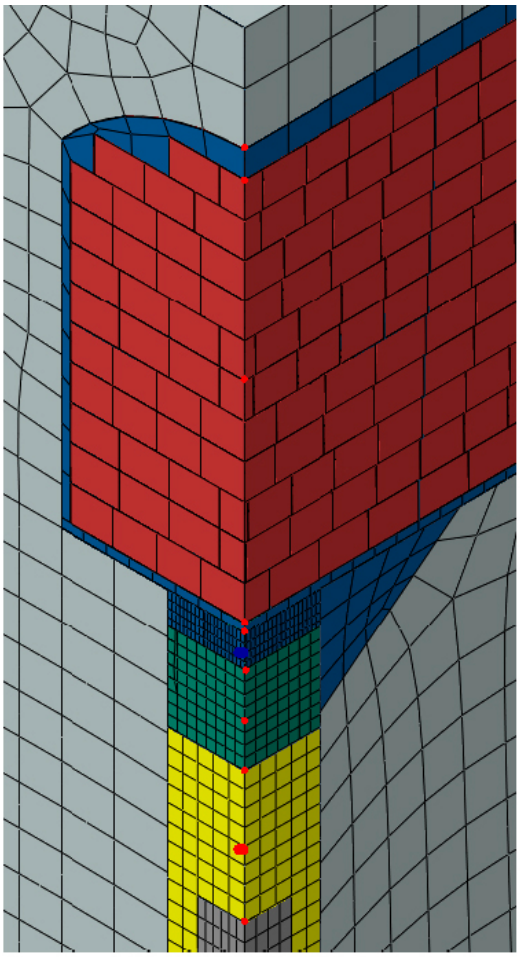

Figure 5-3. *Location of points for history plots of vertical displacements.*

5.6.1 Influence of the design and properties of the bottom bed

General

The problems with convergence made it impossible to run the problems with the expected stiffness of the pellets filling in the floor (corresponding to compacted and uncompacted filling) and in the upper parts of the deposition hole. This was mainly caused by the large compression and subsequent deformations that occur in the pellets filling in combination with the complicated interaction with the pellet filling in the bevel. However if the stiffness was increased to an E-modulus that is double the expected E-modulus of a compacted pellets filling the calculation was successful. This case corresponds to the case named stiffer with

E_3 = 20 MPa

The other calculations with lower stiffness of the pellet filling could only be completed after removal of the bevel by replacing it with rock. A number of calculations with different stiffness of the pellets filled parts have been done including one calculation with the same stiffness (stiffer) as the successful calculation with bevel. Since the two calculations with stiffer pellets yielded very similar results the conclusion is that the results without bevel can be used. The insignificant influence of the bevel in the dry case is rather logical since the upper bentonite blocks in the deposition hole are just moving upwards opposed to the wet case were it swells radially into the bevel.

Very stiff pellet filling with bevel

The results of the one successful calculation with bevel are shown in Figures 5-4 to 5-9 (*blocks_simplified_stiffer_1d_55*). Figure 5-4 shows the upwards swelling for different nodes above the canister. The total maximum swelling of the buffer is 92 mm. The figure also shows that the swelling is completed after $4 \cdot 10^9$ seconds or 127 years. However, as stated earlier the time scale is extended by the damping forces and not very relevant.

The rest of the figures show the end state. Figures 5-5 and 5-6 show contour plots of the vertical displacements in the model. Figure 5-7 shows the lateral displacements. Figure 5-8 shows the distribution of the vertical stresses. The final distribution of swelling pressure, void ratio and density at saturation are shown in Figure 5-9. The code uses void ratio for the calculations and this variable can be converted to density.

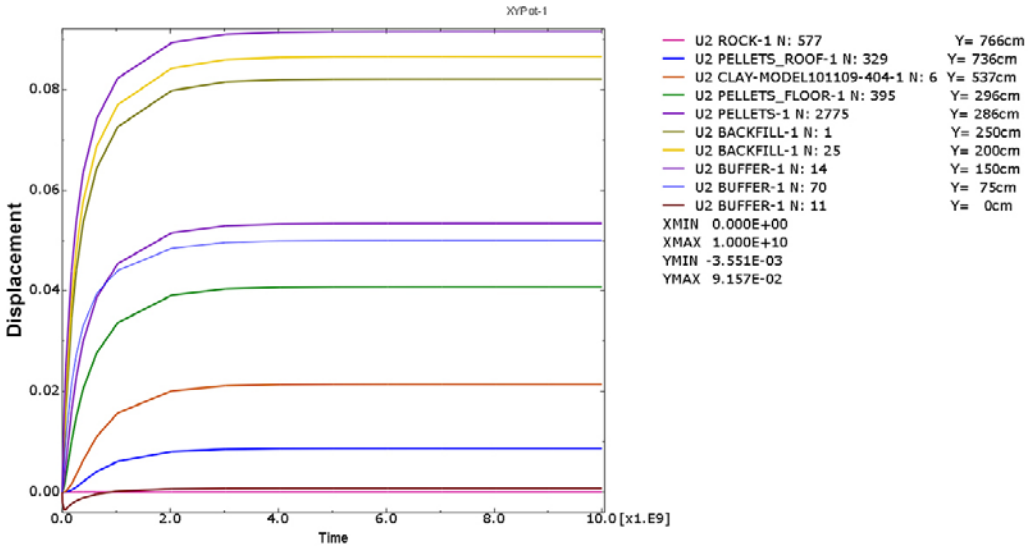

Figure 5-4. *Upwards displacements (m) vs. time (s) of different nodes in the vertical centre line of the deposition hole. Y=distance from canister top.*

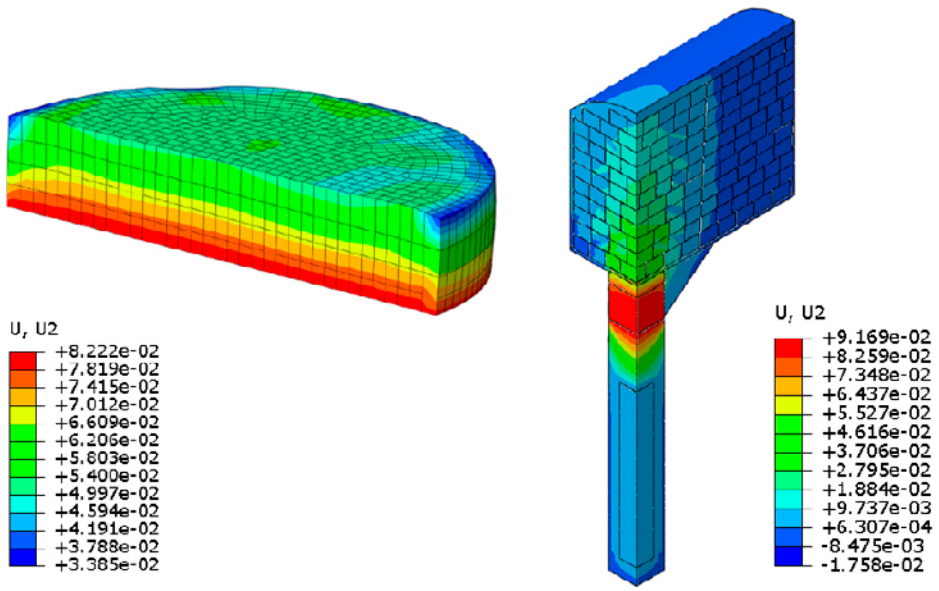

Figure 5-5. *Contour plots of upwards swelling (m) of the pellets filling in the upper part of the deposition hole with the bevel to the right (left) and in a large part of the model.*

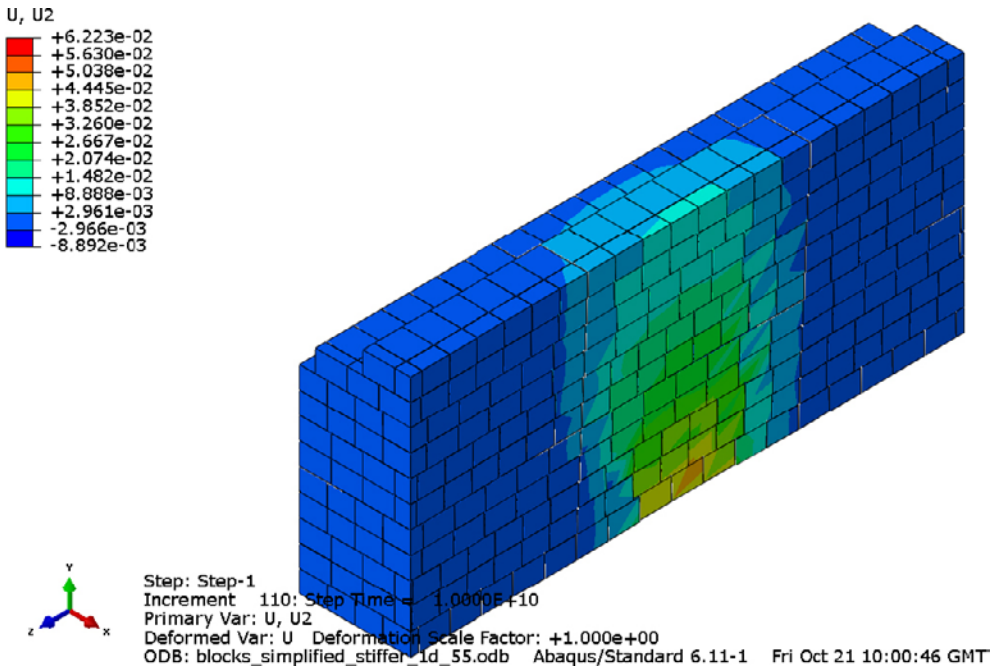

Figure 5-6. *Upwards swelling (m) of the backfill blocks.*

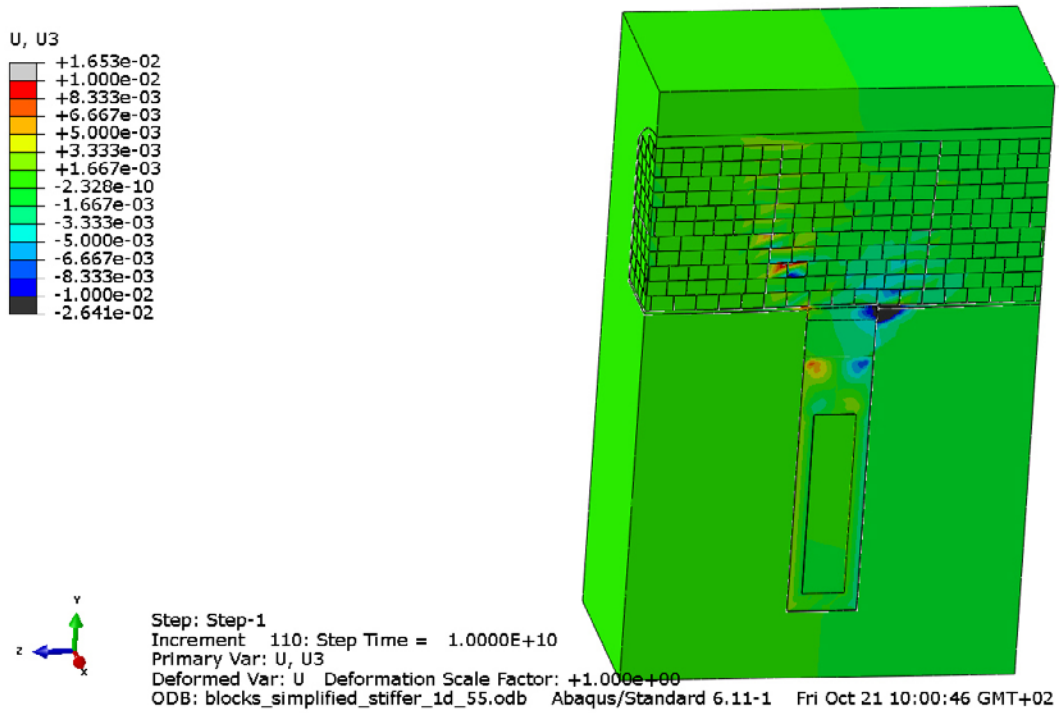

Figure 5-7. *Sideways swelling (m).*

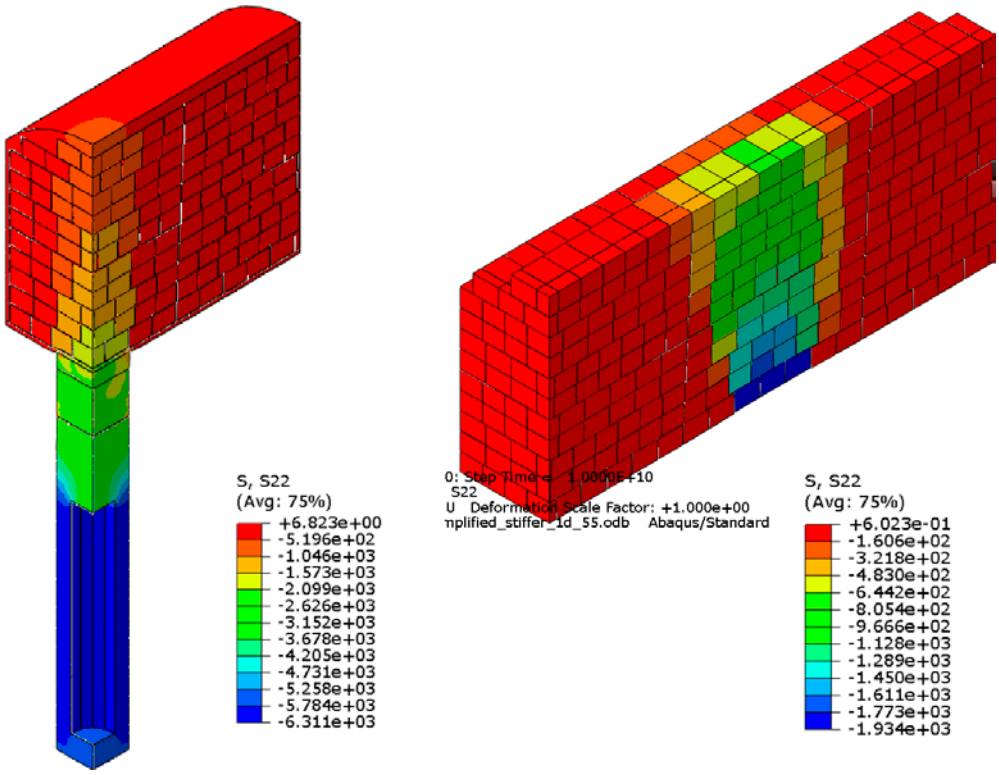

Figure 5-8. *Vertical total stress (kPa) in the deposition hole and in the blocks.*

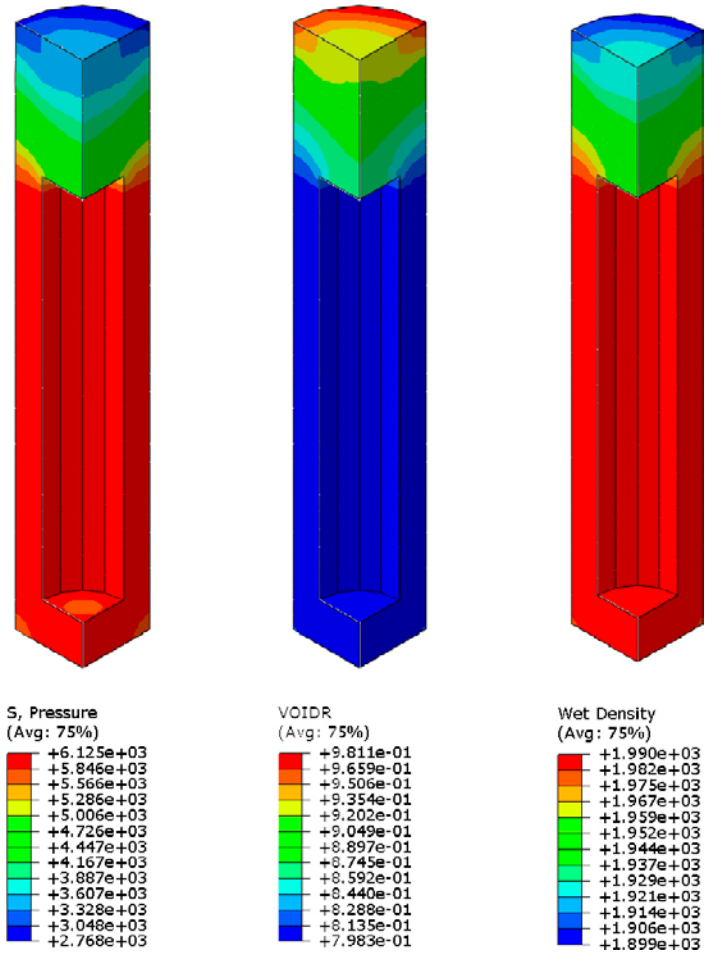

Figure 5-9. *Average stress (kPa), void ratio and density at saturation (kg/m^3) in the bentonite buffer.*

The figures show that

- A large part of the total compression of about 9 cm takes place in the pellets filling in the deposition hole and in the bottom bed (4–5 cm).
- A large part takes place in the backfill block part (about 3 cm).
- The rest takes place in the pellet filling in the roof (about 1 cm) and in the backfill blocks in the deposition hole (about 1cm).
- There is a lateral displacement of the pellet filling in the deposition hole into the pellets filling in the bevel of about 2.5 cm.
- There is a lateral stress spreading caused by the overlapping block masonry, which in combination with the friction reduces the vertical stress from about 1.9 MPa at the contact between the blocks and the bottom bed to about 0.6 MPa at the contact between the blocks and the pellets filling in the roof.
- The swelling pressure is about 4.5 MPa and the density at saturation on top of the canister is 1,950 kg/m^3, i.e. the criteria is fulfilled for this case.

The modelling results of this case thus show that the upwards swelling and subsequent density loss of the buffer is acceptable, but the margin is not very large in spite of the stiff pellet filling.

Simplified case without bevel

Since the calculations with a bevel were not successful for the cases with normal pellets stiffness, the element mesh was changed and the bevel removed. The influence of the bevel was checked by repeating the calculation with bevel, were very stiff pellet filling was used, with the element mesh without bevel.

Figure 5-10 shows the modified element mesh. The properties of the bevel have been changed to those of the rock and is defined as part of the rock and thus no contact definition is required between the bevel and the original rock surface. Contact elements with no friction were assigned between the cylindrical pellets filling in the deposition hole and the rock.

Four calculations with different pellet stiffness have been performed as shown in Table 5-4.

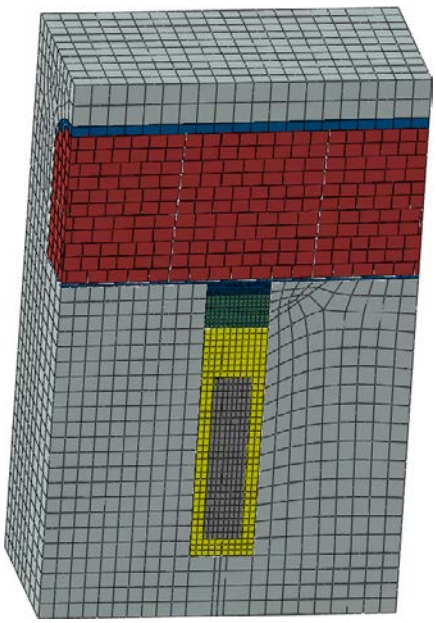

Figure 5-10. *Modified element mesh used in the simplified model without bevel.*

Table 5-4. Calculations done in the model without bevel.

Name	E-modulus of bottom bed and pellets in dep.hole	E-modulus of pellets at the roof and walls
Uncompacted filling (1c_55)	3.9 MPa	3.9 MPa
Compacted filling (stiff_1c_55)	10 MPa	10 MPa
Compacted floor (stiff_floor_1c_55)	10 MPa	3.9 MPa
Very stiff filling (stiffer_1c_55)	20 MPa	20 MPa

Very stiff filling

This calculation was done with the E-modulus 20 MPa for comparison with the same calculation with bevel.

Figures 5-11 to 5-13 show some results.

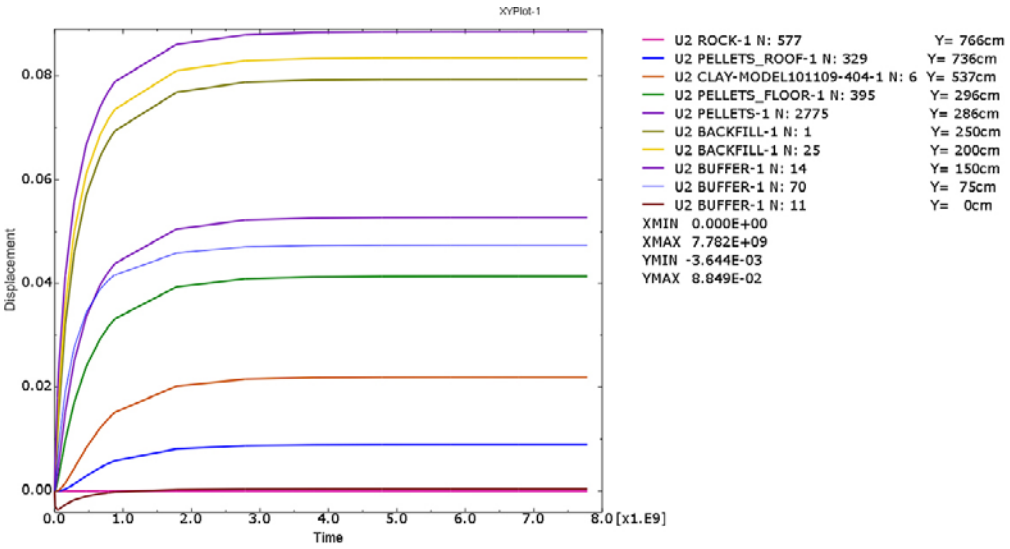

Figure 5-11. *Upwards displacements (m) vs. time (s) of different nodes in the vertical centre line of the deposition hole. Y = distance from canister top.*

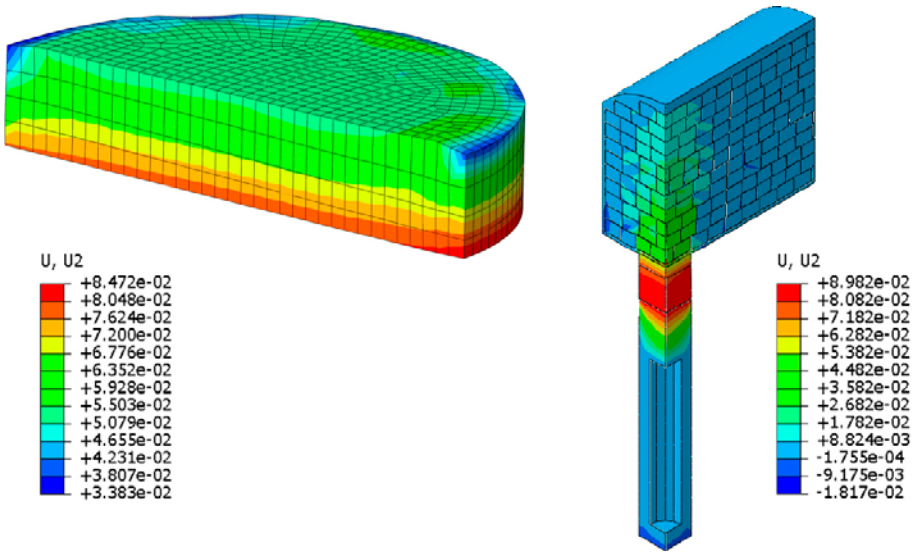

Figure 5-12. *Contour plots of upwards swelling (m) of the pellets filling in the upper part of the deposition hole (left) and in a large part of the model.*

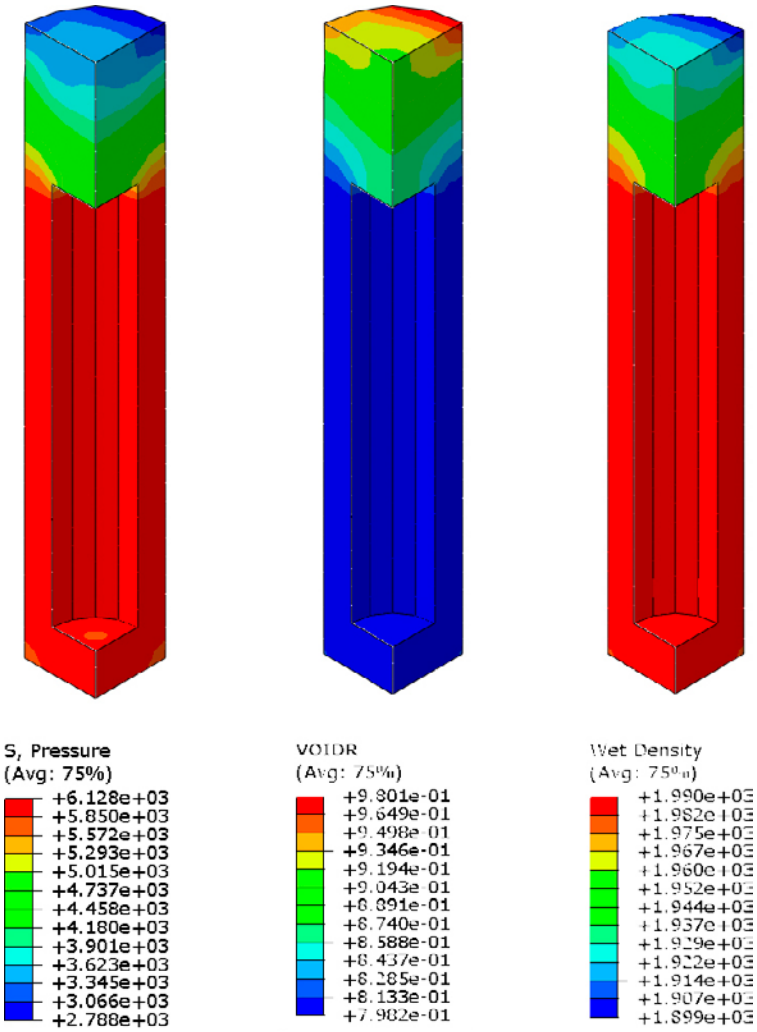

Figure 5-13. *Average stress (kPa), void ratio and density at saturation in the bentonite buffer.*

Comparing the results of the calculations with very stiff pellets filling (E = 20 MPa) show that

- The upwards swelling of the buffer is about 3% lower for the simplified model.
- The swelling pressure and density at saturation on top of the canister are almost identical.

The conclusion is thus that the difference is so small that a simplified model can be used for the dry case.

Uncompacted filling

Some results of the calculation with the uncompacted pellets fillings are shown in Figures 5-14 to 5-18. It is interesting to compare this calculation with the ones with very stiff pellets filling. The total maximum swelling (Figure 5-14) of the buffer is 164 mm. The figure also shows that the swelling takes longer time and is completed after $7 \cdot 10^9$ seconds or 222 years, which is logical due to the larger swelling. However, as stated earlier the time scale is extended by the damping forces and not very relevant.

Interesting observations are (the results of the very stiff pellets calculation are shown within parenthesis for comparison):

- A larger part of the total compression of about 16 (9) cm takes place in the pellets filling in the deposition hole and in the bottom bed (about 12 (4) cm).
- A small part takes place in the backfill block part (about 2 (3) cm).
- The rest takes place in the pellet filling in the roof (about 2 (1) cm).

- There is a lateral stress spreading caused by the overlapping block masonry, which in combination with the friction reduces the vertical stress from about 1.2 (1.9) MPa at the contact between the blocks and the bottom bed to about 0.3 (0.6) MPa at the contact between the blocks and the pellets filling in the roof.
- The swelling pressure is about 3.2 (4.5) MPa and the density at saturation 1,920 (1,950) kg/m^3, i.e. the criteria is not fulfilled for this case.

It is interesting to note that the entire increase in compression of the backfill takes place in the pellets filled parts. In fact the compression of the backfill block parts is smaller in the case with soft pellets filling since the vertical stress on the blocks is lower.

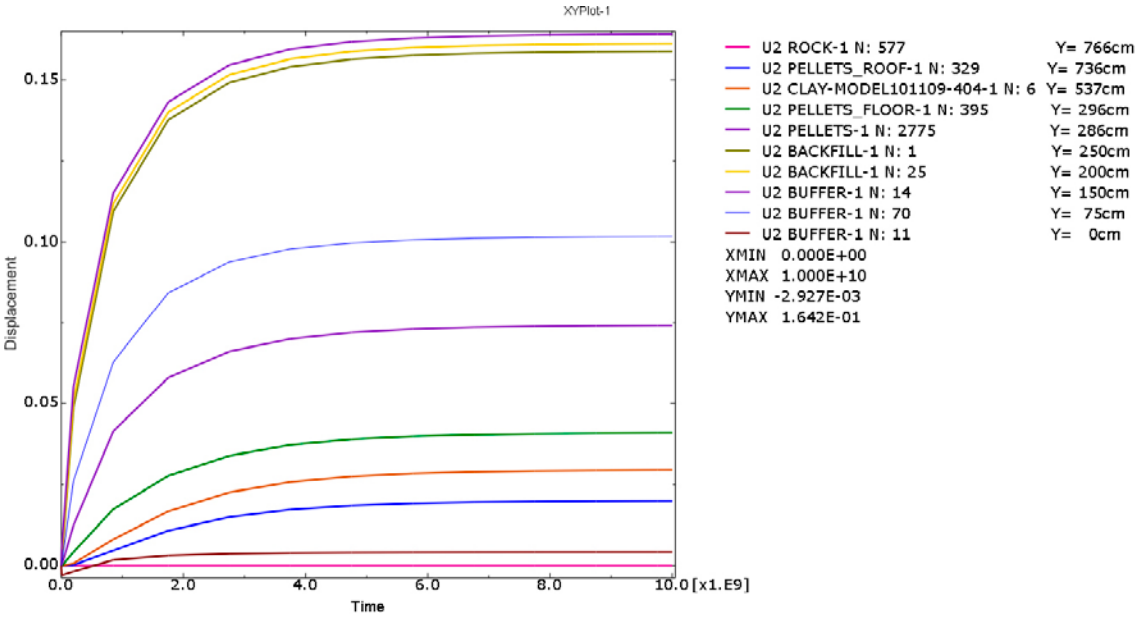

Figure 5-14. *Upwards displacements (m) vs. time (s) of different nodes in the vertical centre line of the deposition hole. Y = distance from canister top.*

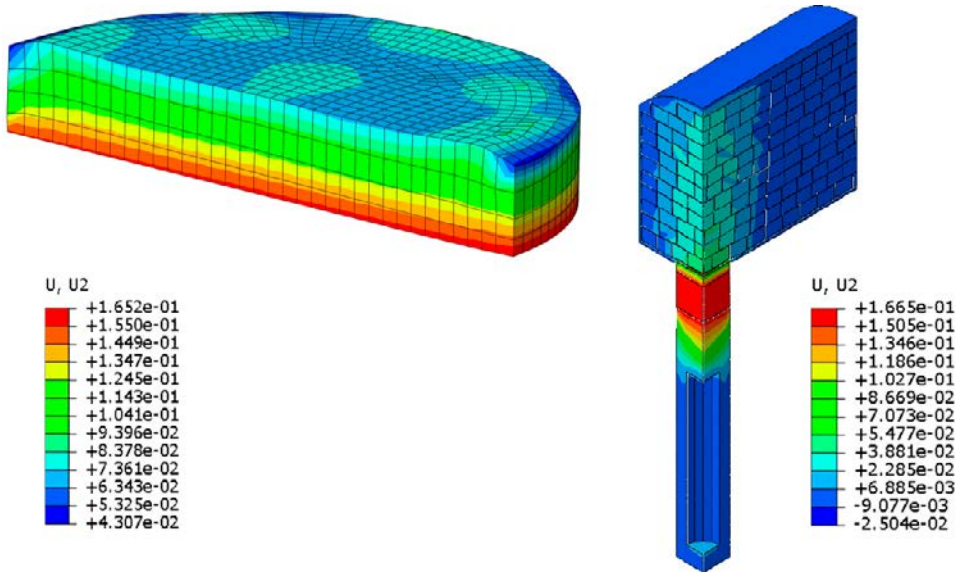

Figure 5-15. *Contour plots of upwards swelling (m) of the pellets filling in the upper part of the deposition hole (left) and in a large part of the model.*

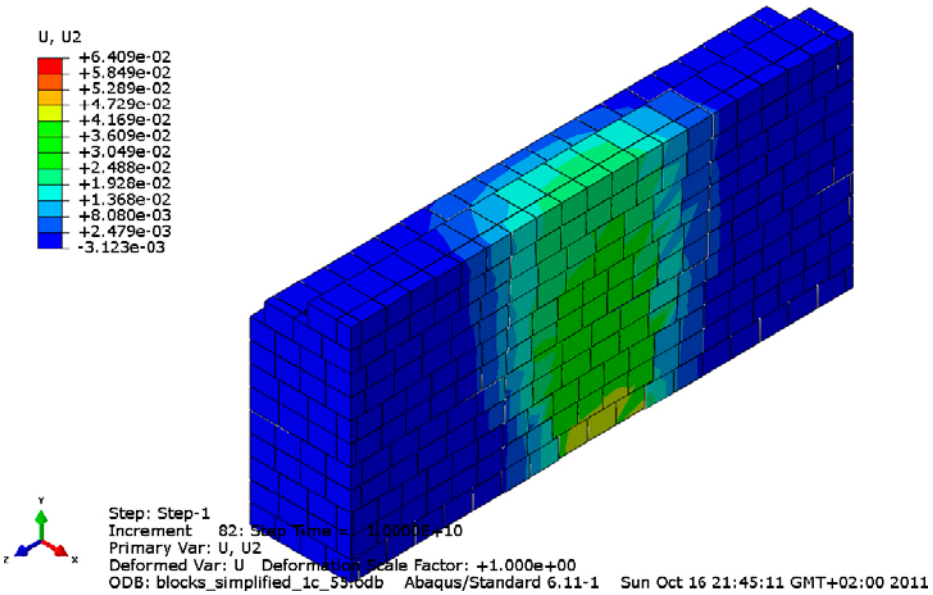

Figure 5-16. *Upwards swelling (m) of the backfill blocks.*

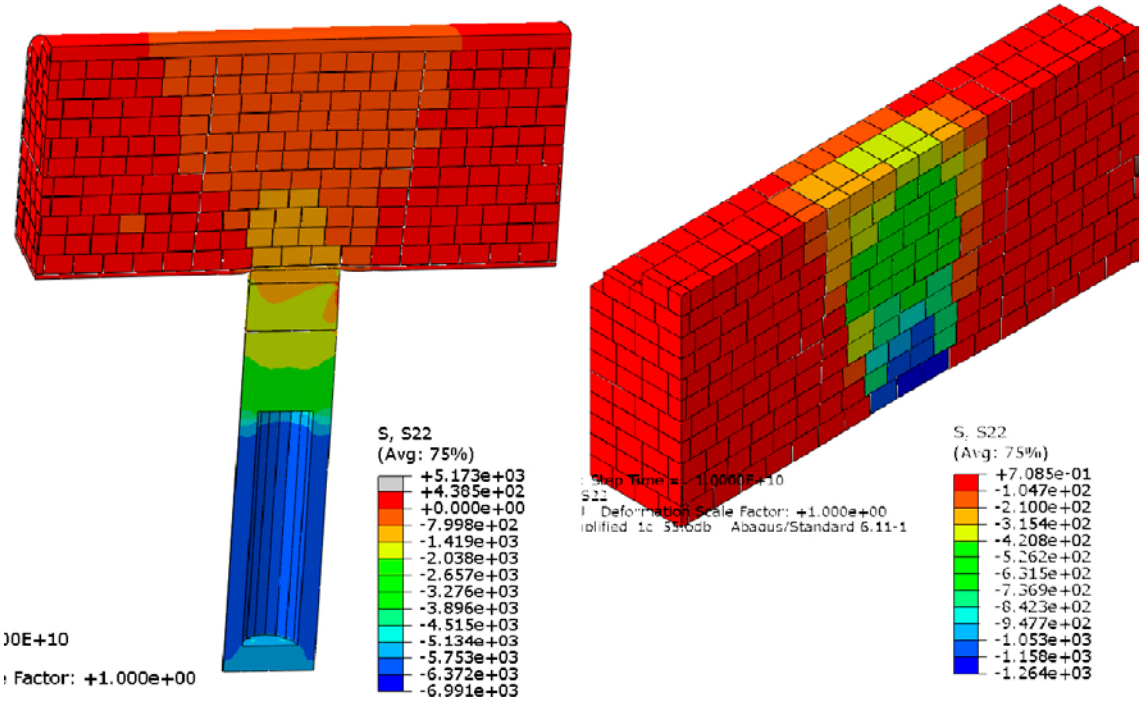

Figure 5-17. *Vertical total stress (kPa) in the deposition hole and in the blocks.*

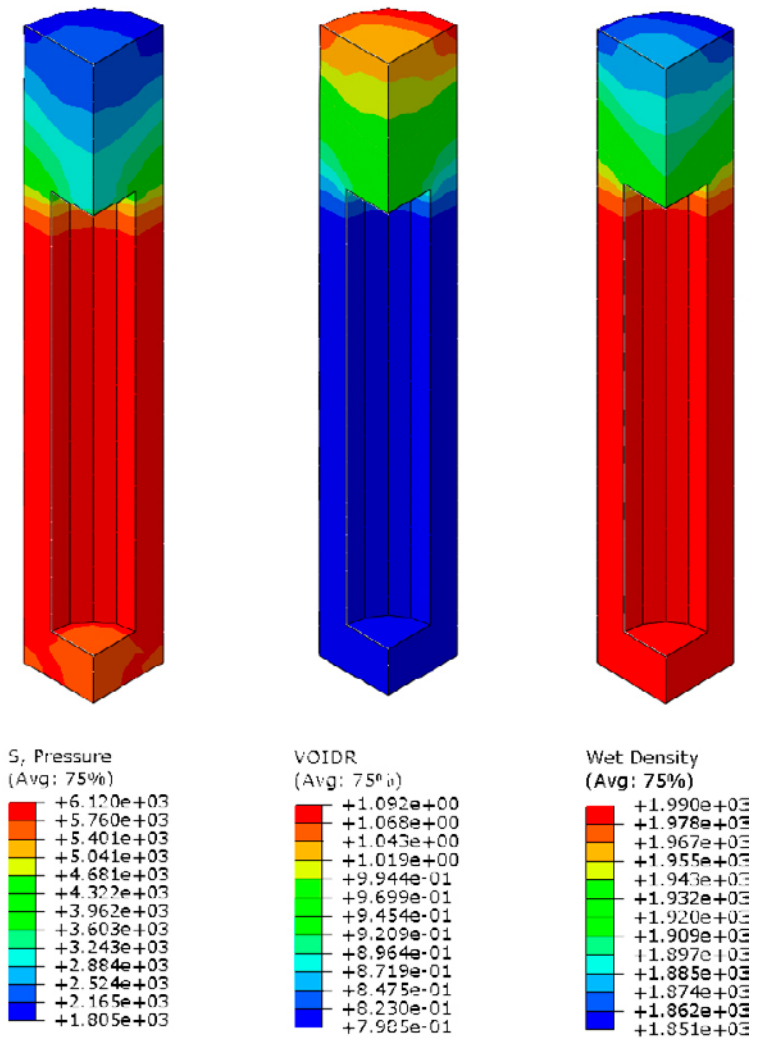

Figure 5-18. *Average stress (kPa), void ratio and density at saturation in the bentonite.*

Compacted filling

This calculation corresponds to the case with compacted pellets filling (E = 10 MPa). Figures 5-19 to 5-21 show some results.

The results from this calculation are as expected between the results of the other two. The total swelling of the buffer is about 11 cm and the density at saturation on top of the canister 1,940 kg/m^3 and does thus not fulfil the criteria.

Compacted floor

Since it is not likely that the pellets filling at the roof can be compacted one calculation with compacted pellets in the floor and in the upper part of the deposition hole (E = 10 MPa) and uncompacted pellets at the roof (E = 3.9 MPa) has been performed. Figures 5-22 to 5-24 show the same results as for the other calculations.

The results from this calculation do not differ very much from the one with compacted pellets filling also at the roof. The total swelling of the buffer is about 12 cm and the density at saturation on top of the canister 1,935 kg/m^3 and does thus not fulfil the criteria. The influence of the stiffness of the pellets filling at the roof is small compared to the influence of the stiffness of the pellets filling beneath the backfill blocks. This calculation can also be compared with the older calculation named Model 1 summarised in Table 2-2, the main difference being the thickness of the pellet filling under the backfill blocks. In the old calculation with a small thickness of the pellet filling (8 cm) the density criteria was fulfilled in opposite to in the design with pellet filling in the top of the deposition hole.

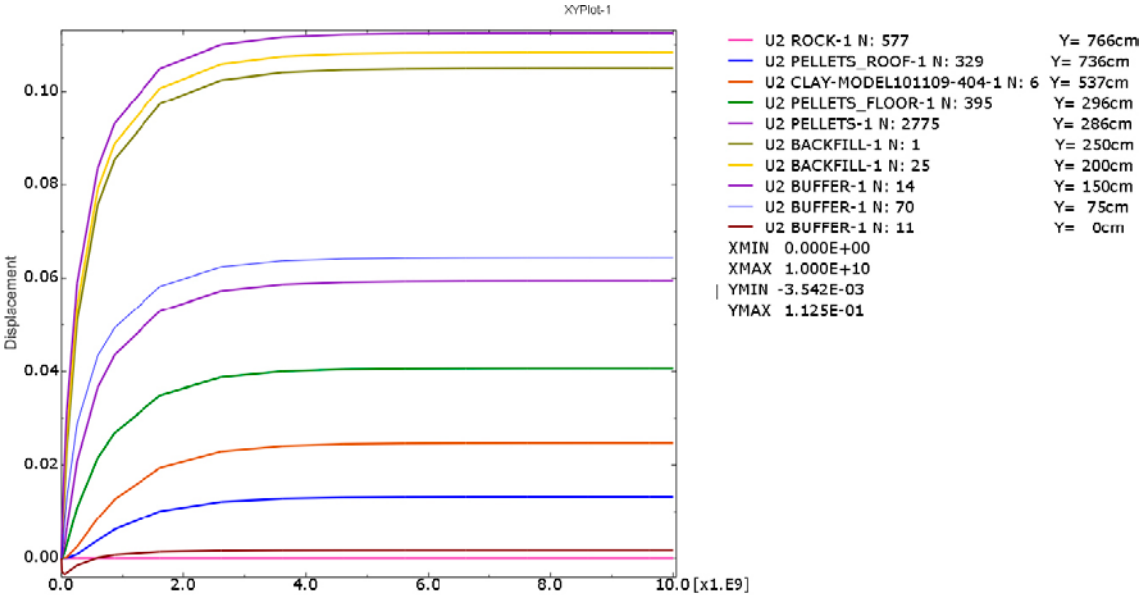

Figure 5-19. *Upwards displacements (m) vs. time (s) of different nodes in the vertical centre line of the deposition hole. Y = distance from canister top.*

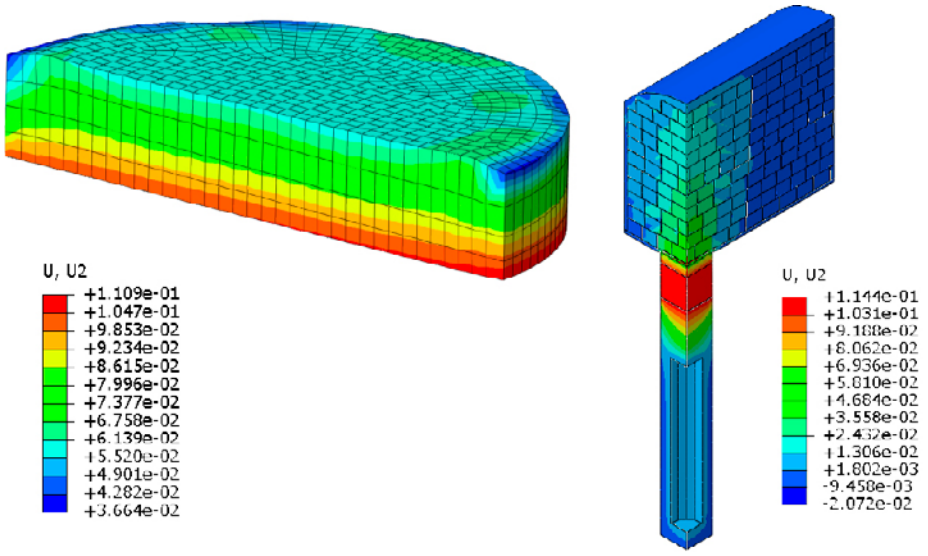

Figure 5-20. *Contour plots of upwards swelling (m) of the pellets filling in the upper part of the deposition hole (left) and in a large part of the model.*

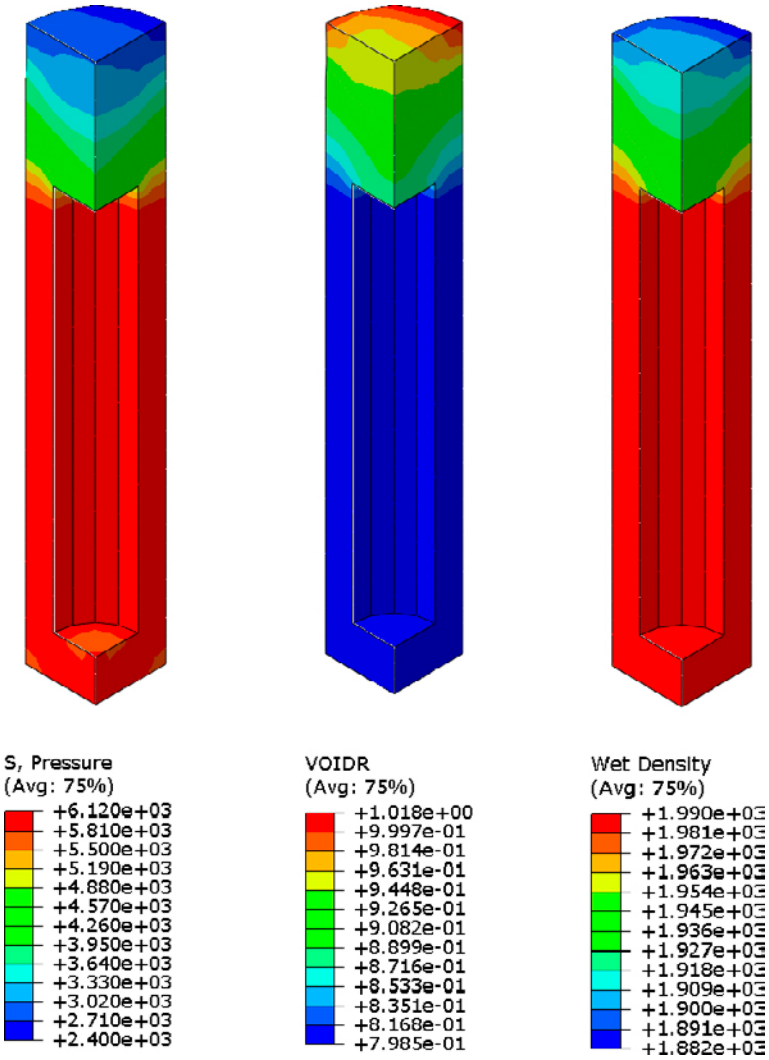

Figure 5-21. *Average stress (kPa), void ratio and density at saturation in the bentonite buffer.*

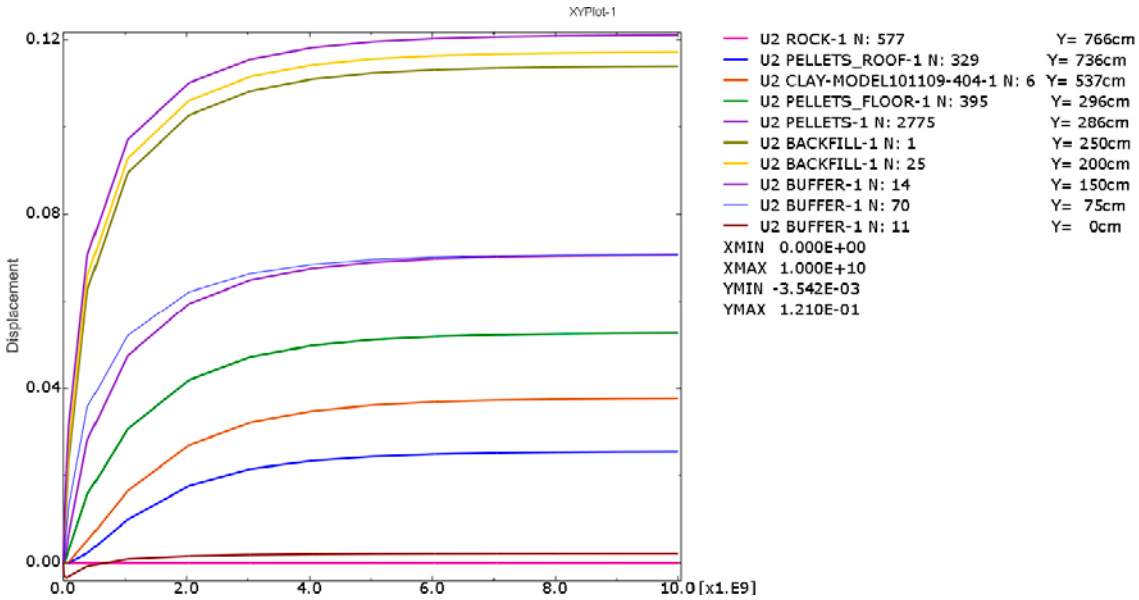

Figure 5-22. *Upwards displacements (m) vs. time (s) of different nodes in the vertical centre line of the deposition hole. Y = distance from canister top.*

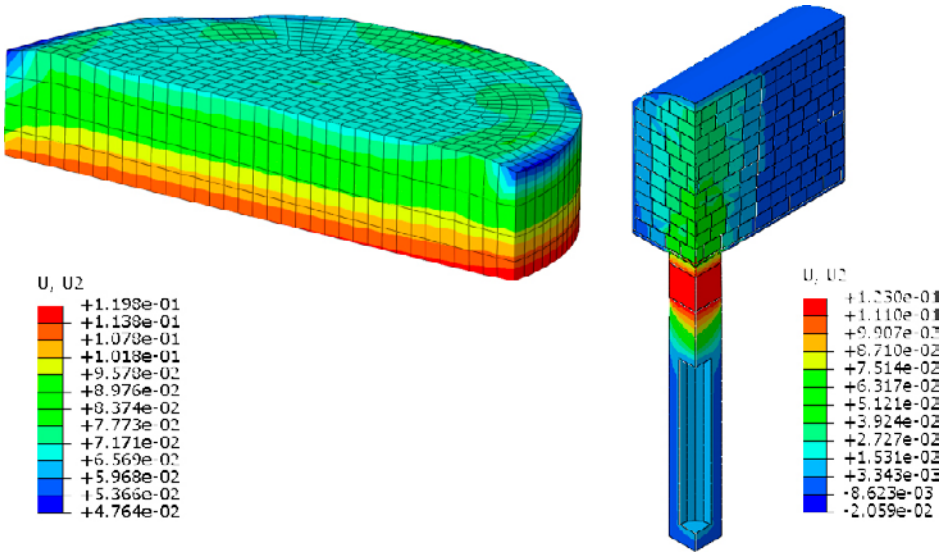

Figure 5-23. *Contour plots of upwards swelling (m) of the pellets filling in the upper part of the deposition hole (left) and in a large part of the model.*

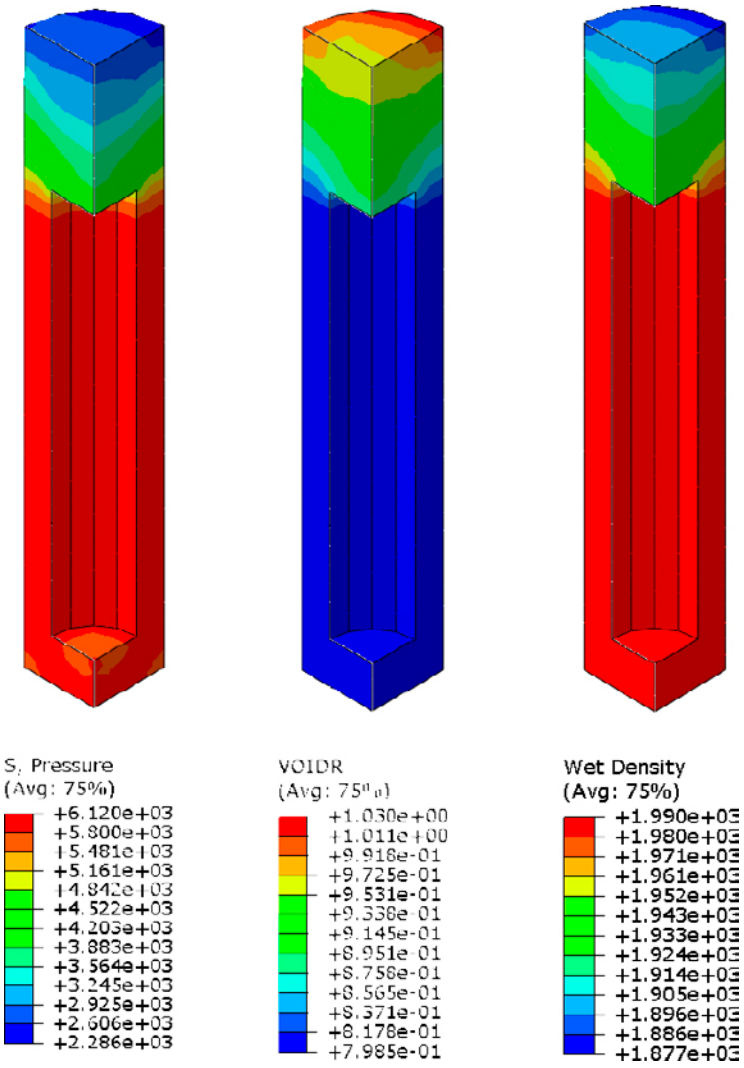

Figure 5-24. *Average stress (kPa), void ratio and density at saturation in the bentonite buffer.*

Comparison of results and some conclusions

Some of the results of the five calculations shown are compiled in Table 5-5.

A comparison between different models shows some interesting things:

- The influence of the bevel on the upwards swelling is very small in the dry case. This is very logical since the bevel does not interact with the backfill blocks in the deposition hole and the interaction with the bottom bed is limited due to the limited height of the bottom bed. The very small influence of the bevel is of course caused by the assumption that the backfill blocks are unaffected by wetting. If also these would be assumed to be completely water saturated the results would be quite different.
- The properties and thus also the thickness of the bottom bed are dominating the upwards swelling.
- Also the properties of the pellet filling at the roof has some influence but not very strong.
- The compression of the backfill block section in the tunnel is quite large which is caused by the properties of the slots between the blocks.
- The uncompacted pellets fillings with low E-modulus yield too large swelling, which violates the density criteria.
- Also the compacted pellet filling yields too large swelling.

Although the number of calculations is limited it would probably be possible to estimate the effect of additional changes in properties and dimensions of the pellets fillings and the block gaps by interpolation or analytical treatment, but this has not been done since the density criterion is not fulfilled for any of the realistic cases.

5.6.2 Influence of the pellets filling at the roof

The influence of the pellet filling at the roof is investigated partly by the calculations shown in Section 5.6, where different stiffness was used and partly by a calculation where pellet filling in the roof is omitted.

In the latter calculation the element mesh was the same as shown in Figure 5-1, with the exception that there were no contact between the block section and the pellet filling in the roof. There were also some parts of the bevel between the pellet filling in the bevel and the backfill blocks that were missing, which to some extent explain why this calculation with very large swelling was possible to run. The properties of the different materials were the same as calculation “Uncompacted filling” (see Table 5-4).

Table 5-5. Compilation of results.

Calculation	Buffer swelling (mm)	Compression of				Density at canister lid (kg/m^3)
E-modulus of pellets in bottom/roof		backfill blocks in dep. hole (mm)	pellets in bottom filling* (mm)	backfill blocks in tunnel (mm)	pellets top filling (at roof) (mm)	
Bevel E = 20/20 MPa	92	10	41	32	9	1,950
No bevel E = 20/20 MPa	89	10	38	32	9	1,950
No bevel E = 10/10 MPa	113	8	64	28	13	1,940
No bevel E = 10/3.9 MPa	121	8	61	26	26	1,935
No bevel E = 3.9/3.9 MPa	164	6	116	23	19	1,920

*both in deposition hole and tunnel

The calculation did not converge to a final stage, but was run far enough to draw conclusions about this case. Figure 5-25 shows the element mesh and the vertical displacements at the end of the calculation.

Figure 5-26 shows the upwards swelling as function of time and Figure 5-27 shows the void ratio in the upper part of the buffer at the end of the calculation *(blocks_tunnel_2c_small2_v683)*.

The results clearly shows that in spite of that the swelling is not finished the swelling is very large (about 35 cm) and the resulting void ratio at the top of the canister very high (1.15), corresponding to a density at saturation of 1,830 kg/m^3, which is far from acceptable.

The influence of the thickness of the pellet filling at the roof can be done by comparing the results in Section 5.6.1. The two calculations "Compacted filling" and "Compacted floor" show almost double compression of the pellet filling at the roof from 14 mm to 26 mm at a more than halving of the stiffness of the filling from 10 MPa to 3.9 MPa yielding a decrease in buffer density above the canister with 5 kg/m^3. A doubling of the thickness of the slot in the roof from 30 cm to 60 cm is estimated to yield similar effect i.e. a decrease in density above the canister with 5 kg/m^3.

The conclusion is thus that the voids at the roof must be filled with pellets and that a slot at the roof that is 0.6 m instead of 0.3 m, yields a decrease in buffer density above the canister with 5 kg/m^3.

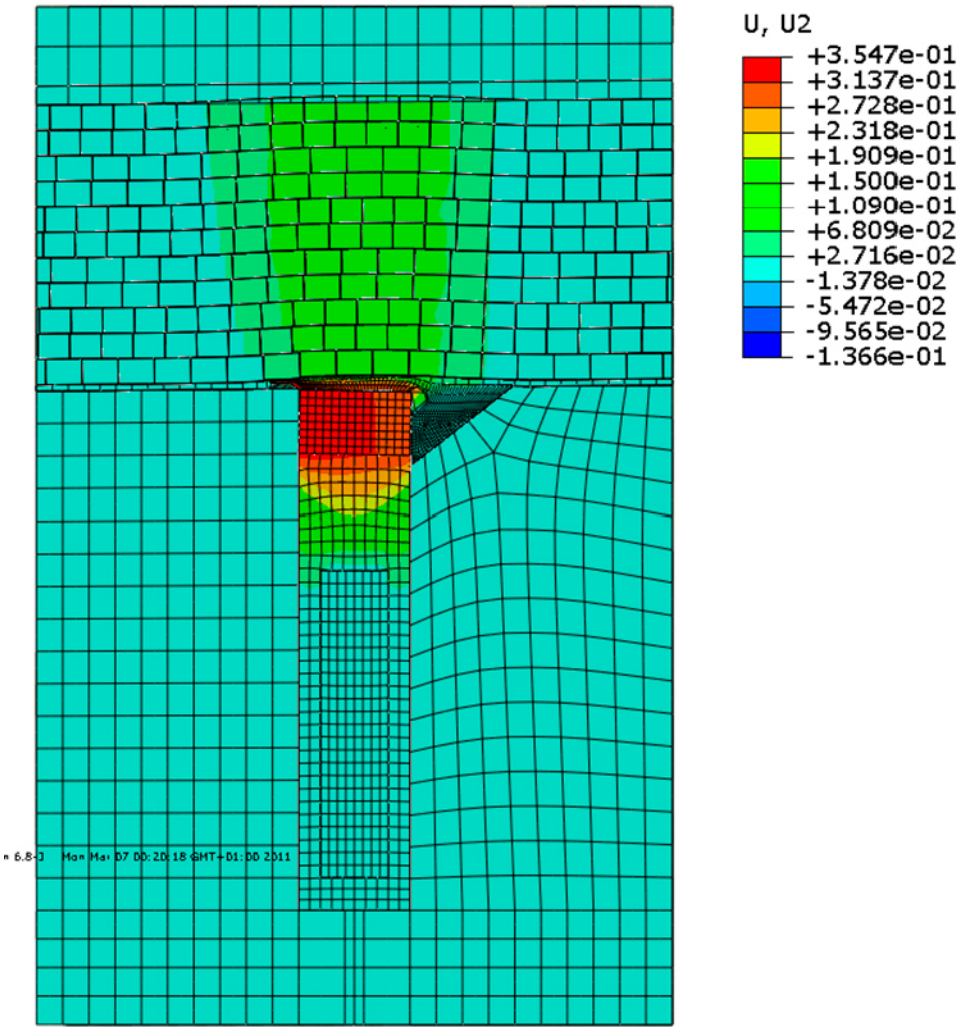

Figure 5-25. *Vertical displacements (m) in the calculation with no pellet filling at the roof.*

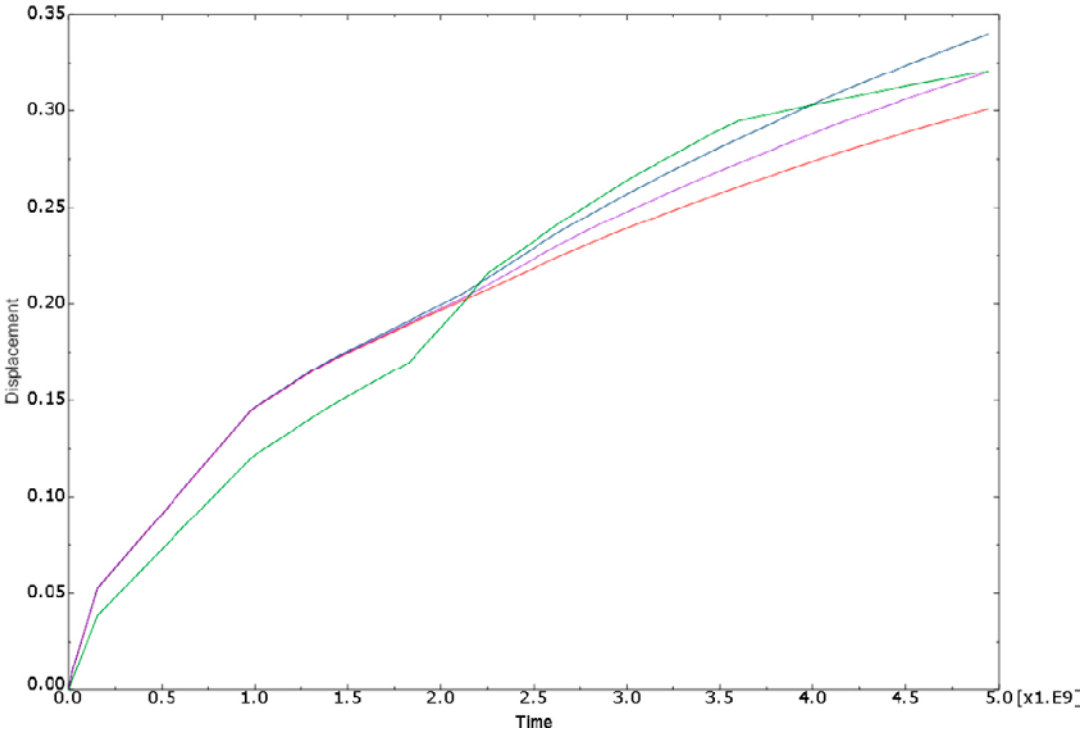

Figure 5-26. *illustration of the upwards swelling (m) of four points in the buffer top as a function of time (s).*

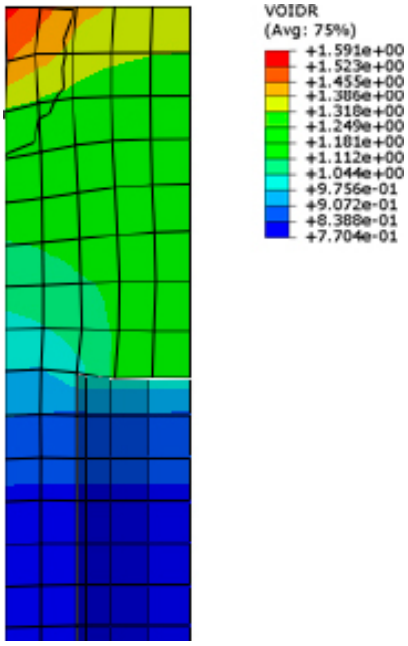

Figure 5-27. *Void ratio e in the upper left part of the buffer at the end of the calculation without pellet filling at the roof. e = 0.77 corresponds to wet density ρ_m = 2,006 kg/m^3 and e = 1.59 corresponds to wet density ρ_m = 1,687 kg/m^3.*

5.7 Conclusions

The overall conclusion from the calculations of the dry case 1A (pellet filling in the top of the deposition hole) is that it yields too low buffer density at the top of the canister when realistic density of the pellet filling is used.

6 Upwards swelling against wet tunnel – case 1B

6.1 General

Case 1B (see Table 3-1) refers to the case with pellets instead of half-block in top of deposition hole and wet backfill. Also the calculation of this case have yielded large problems. Finally two sub-cases have been possible to model. Those sub-cases have a backfill that from start is identical to the buffer with completely homogenised and water saturated backfill with the same density at saturation 2,000 kg/m^3. The only difference between the two sub-cases is the density of the pellet filling.

6.2 Finite element mesh

Figure 6-1 shows the mesh and the property areas of the model. The mesh is similar to the mesh for the dry case but the backfill includes the pellet filling. The backfill (coloured yellow) is modelled with the same simplification as the buffer that is completely homogenised with the same density.

6.3 Material properties

6.3.1 Buffer material

The buffer material is modelled in an identical way as the buffer material of the dry case (see Section 5.3.1).

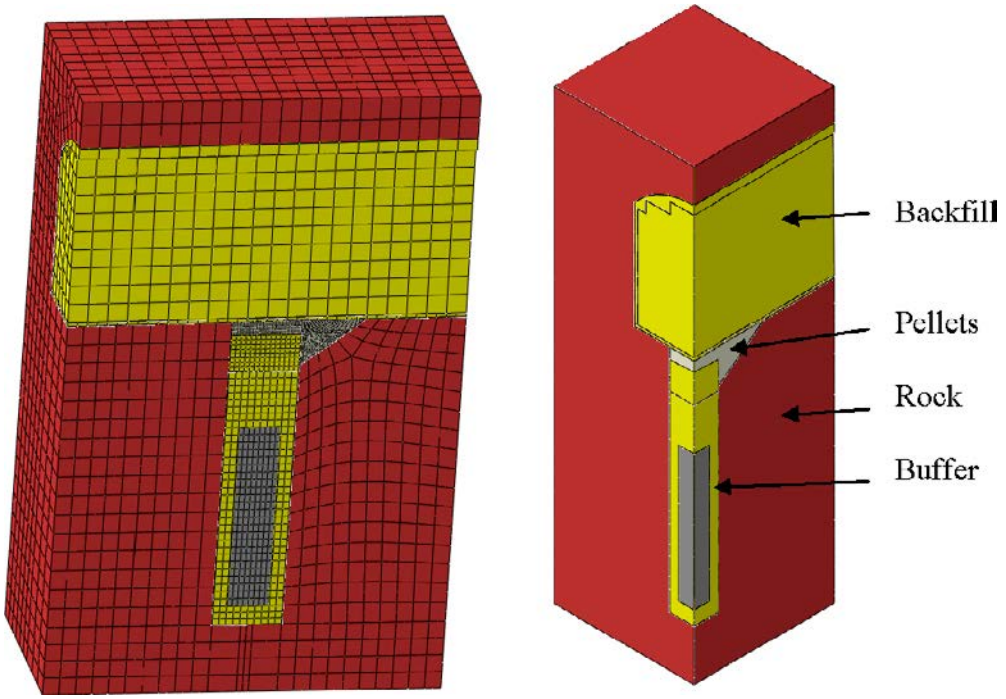

Figure 6-1. *Element mesh and property areas of the wet model. The yellow coloured areas have the same properties.*

6.3.2 Backfill

The backfill has been modelled in an identical way as the buffer (Section 5.3.1), with a density at saturation of 2,000 kg/m^3, which corresponds to the dry density 1,560 kg/m^3. This density corresponds to a degree of block filling in the tunnel of about 82% at the pellet filling dry density of 1,000 kg/m^3 or 78% block filling at the dry density 1,130 kg/m^3 of the pellet filling, which is higher than the expected average values, but may occur locally. According to the production line report (SKB 2010) the average backfill dry density will range between 1,458 and 1,535 kg/m^3.

The material model corresponds to the material model of MX-80, which has a high montmorillonite content and thus higher swelling pressure than a backfill with the lowest acceptable montmorillonite content.

The reasons for choosing the high density and the material model of MX-80 for the backfill are several:

1. Easier to yield converging solutions.
2. Eliminates the upwards swelling into the tunnel backfill since only the pellets filling will be compressed.
3. We don't have a material model for bentonite with low montmorillonite content.

Using such a high density of the backfill is clearly optimistic and the expected results will always be worse. So if this case is not acceptable no other case will be!

6.3.3 Pellet filling

The pellet filling in the bevel and the upper part of the deposition hole is modelled as completely water saturated in contrary to for the dry case were it is modelled as completely dry. The model is the same as the the model of the buffer but the initial conditions differ (identical to how the pellet filling in the buffer was modelled for CRT and SR-Site (Åkesson et al. 2010)). Two different initial densities have been modelled:

Sub-case 1

$u_0 = -50$ kPa

$p_0 = 50$ kPa

$e_0 = 1.78$

This sub-case corresponds to loose filling of the pellets (dry density 1,000 kg/m^3).

Sub-case 2

$u_0 = -300$ kPa

$p_0 = 300$ kPa

$e_0 = 1.40$

This sub-case corresponds to compacted filling of the pellets (dry density 1,158 kg/m^3).

6.3.4 Contact surfaces

The same contact surfaces between the backfill and the rock as between the buffer and the rock have been used i.e.

$\phi = 8.69°$
$c = 0$

This friction angle corresponds to $\beta = 17°$ in the Drucker Prager model.

6.4 Boundary conditions

The mechanical and hydraulic boundary conditions are identical to the boundary condition of the dry case (Section 5.4). The rock surface at the buffer is given free access to water by applying a constant pore water pressure 0 kPa.

6.5 Calculation sequence

See Section 5.5. None of the two cases could be run to complete end, i.e. the pore pressure 0 in the entire model. Also the damping forces were not in complete equilibrium (i.e. 0), but the evaluation of the results indicate that the calculations were run far enough to yield results close to equilibrium.

6.6 Results

6.6.1 Sub-case 1: loose pellet filling in the bevel

The results of the calculations with loose backfill are shown in Figures 6-2 to 6-7. Figure 6-2 shows the upwards displacement of different points above the canister. The figure shows that the maximum displacement of the buffer is 8.8 cm but the displacement of the top part of the backfill blocks in the deposition hole is larger or 10.5 cm. The figure also shows that the swelling has not come to complete stop but also that the swelling is slow and close to equilibrium at the end of the calculation.

That the calculation has stopped before equilibrium is confirmed in Figure 6-3, which shows the pore pressure distribution at the end. The pore water pressure has decreased significantly from the initial 7 MPa but is still almost 1 MPa at some distant parts of the backfill and 300–400 kPa close to the bevel.

Figures 6-4 and 6-5 show contour plots of the upwards swelling at the end of the calculation. The figures show that in addition to the upwards swelling of the buffer and the backfill blocks in the deposition hole there is a downwards swelling of up to 9 cm of the backfill to the pellets filling in the bevel due to the high swelling pressure of the backfill.

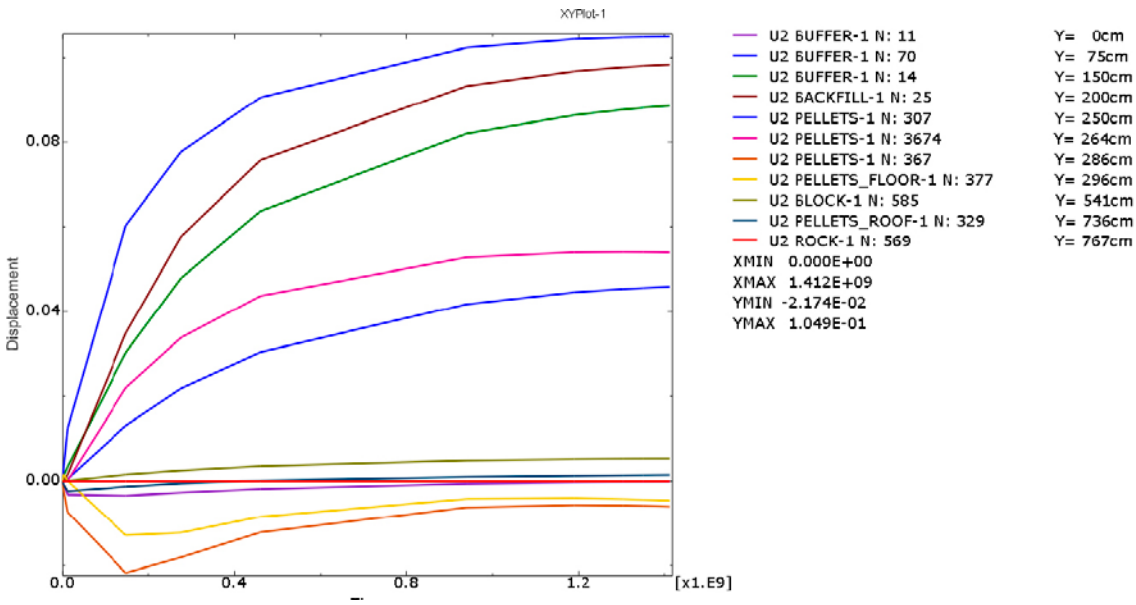

Figure 6-2. *Upwards displacements (m) vs. time (s) of different nodes in the vertical centre line of the deposition hole (see Figure 5-3). Y = distance from canister top.*

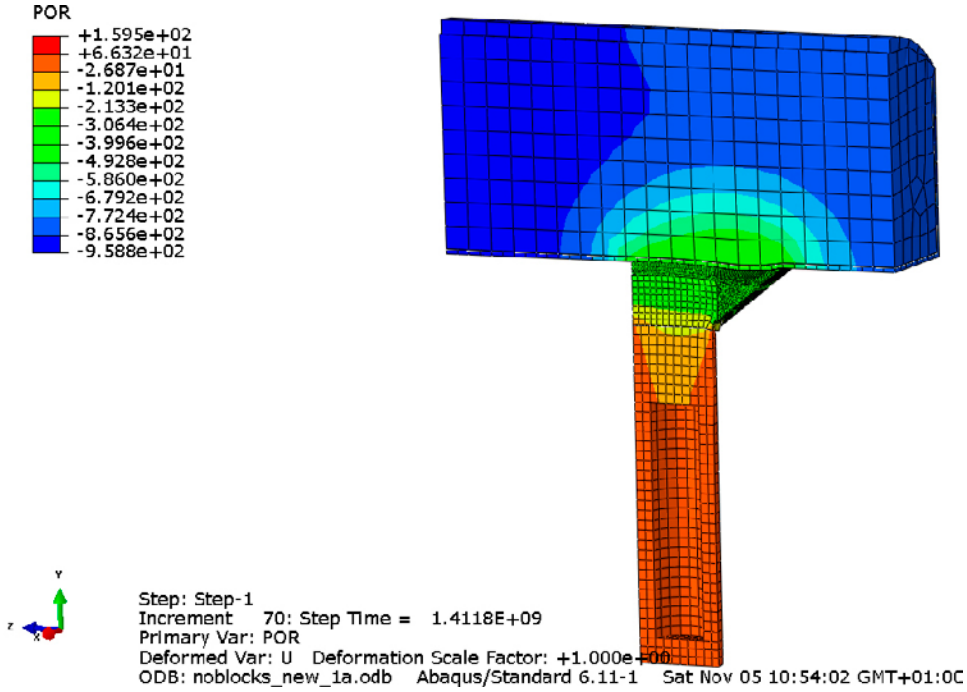

Figure 6-3. *Pore water pressure (kPa) distribution at the end of the calculation.*

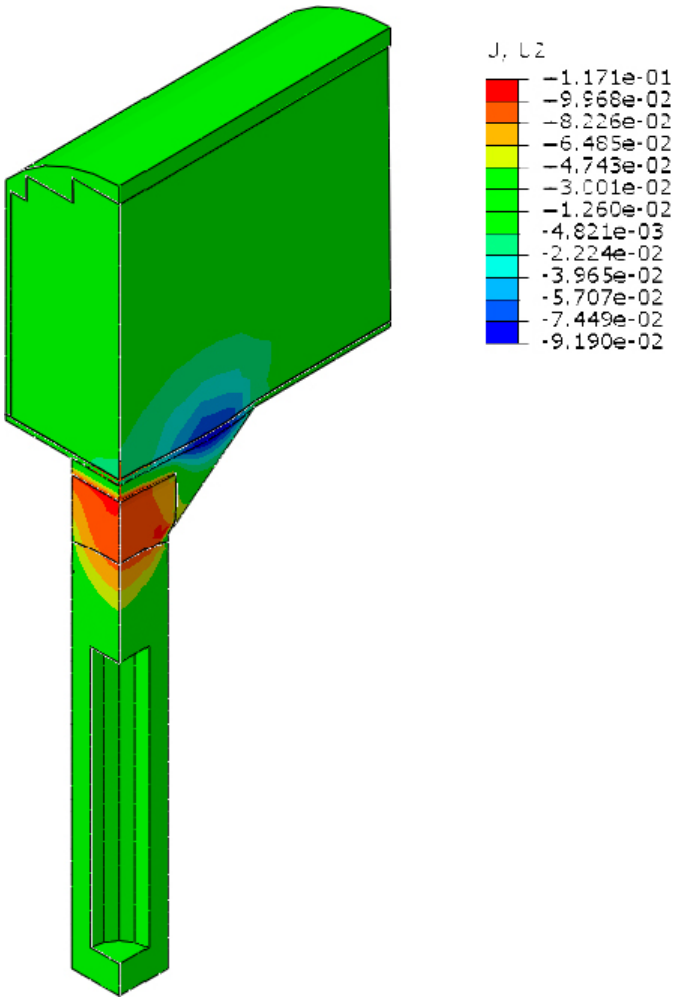

Figure 6-4. *Contour plot of the vertical upwards displacements (m).*

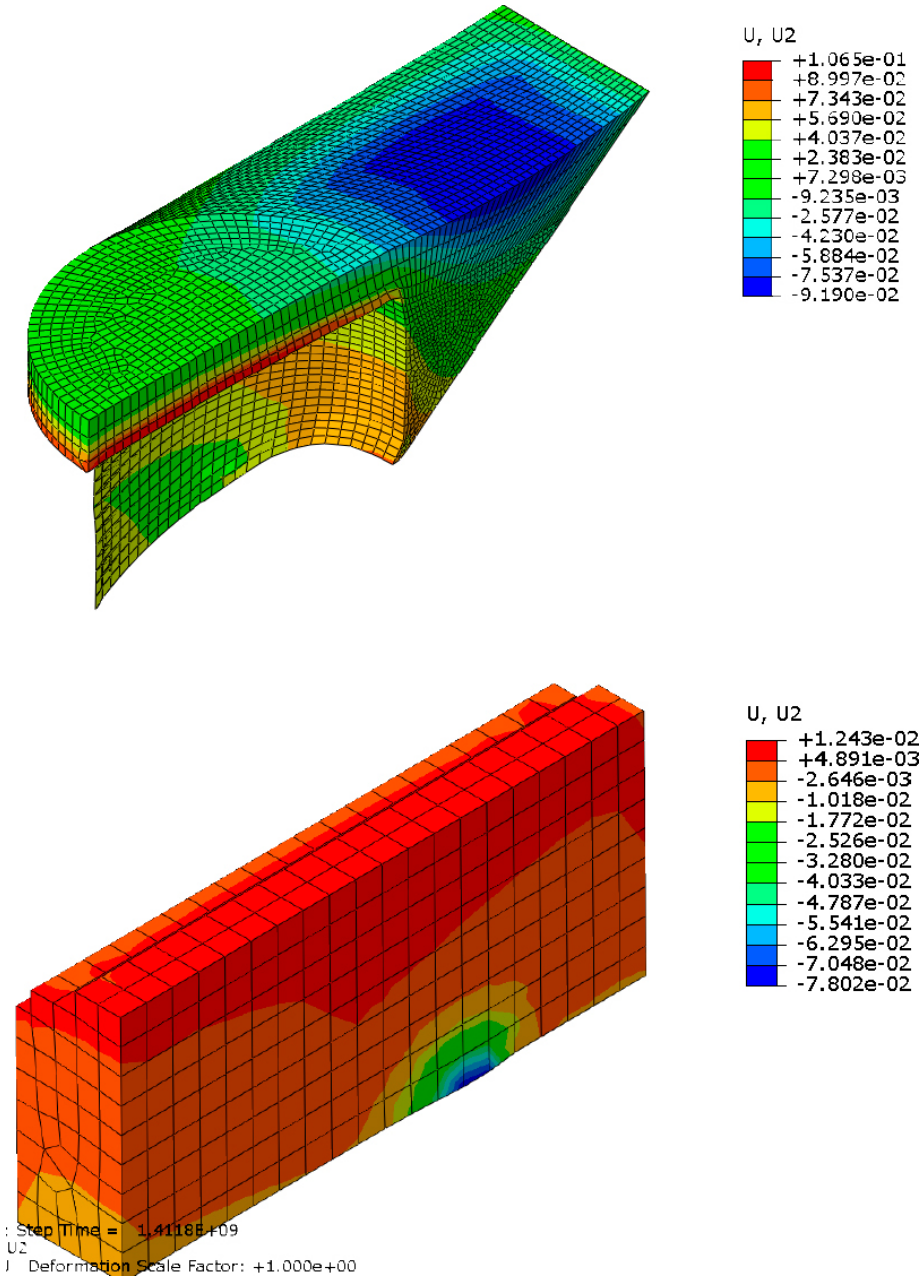

Figure 6-5. *Contour plots of vertical upwards swelling (m) of some details. The upper picture shows the pellets filled parts and the lower picture shows the backfill.*

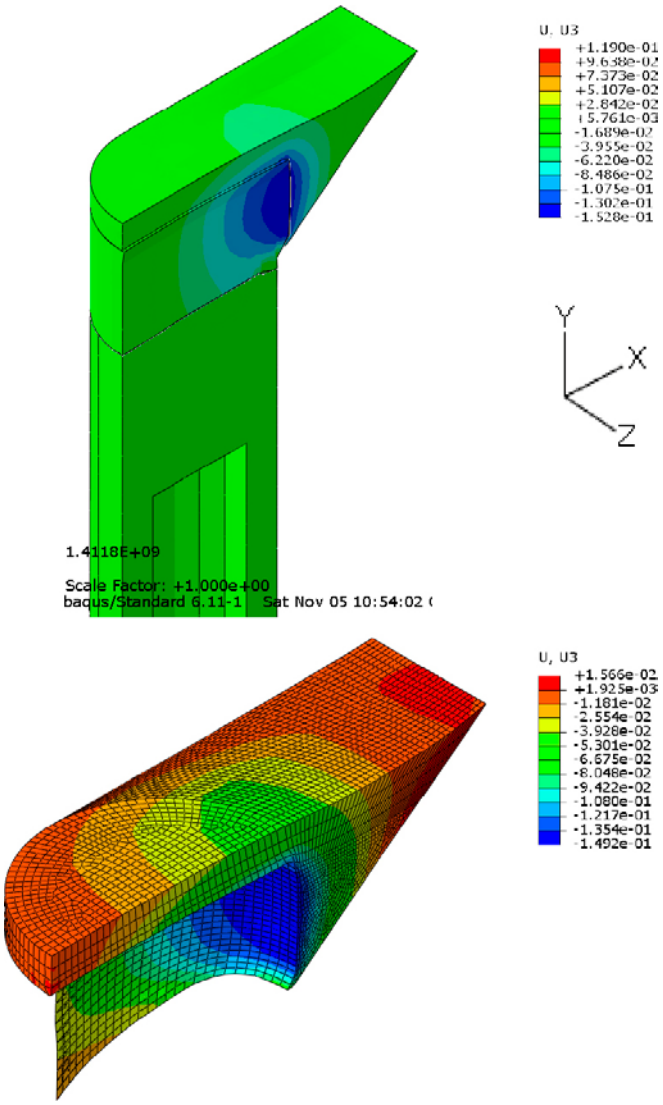

Figure 6-6. *Contour plots of the sideways displacements (m) in x-direction. Only the pellets filling in the bevel and the deposition hole is shown in the lower picture.*

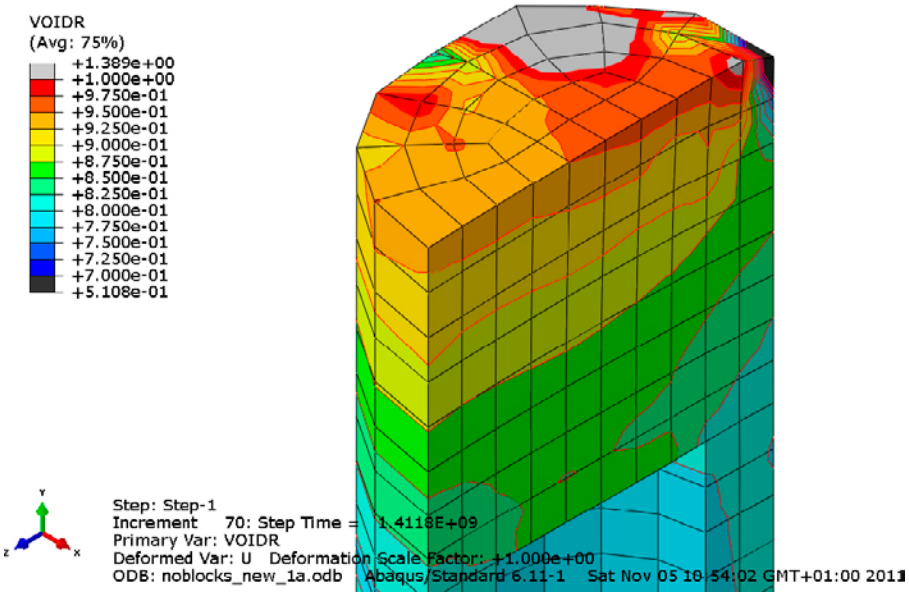

Figure 6-7. *Void ratio in the upper part of the buffer.*

Figure 6-6 shows the sideways swelling. The sideways swelling is quite large and the upper backfill blocks in the deposition hole have swelled more than 15 cm into the bevel.

The void ratio in the buffer is shown in Figure 6-7. The figure shows that the highest void ratio in the buffer above the canister is about 0.86, which corresponds to a density at saturation of 1,950 kg/m^3. This is on the limit of what is accepted. But the figure also shows that the void ratio in the top of the buffer is very uneven with both high and low void ratios. Some corner problems have caused a very low void ratio around the node in that corner. These problems in combination with the fact that the calculation is not completed indicate that there are doubts that the buffer can stand this situation.

6.6.2 Sub-case 2: Compacted pellets filling in the bevel

A higher density of the pellet filling was also modelled in order to see the sensitivity. Identical models were used. The only difference between the calculations was the initial condition of the pellet filling with the void ratio 1.40 (dry density 1,158 kg/m^3) and the swelling pressure 300 kPa instead of 1.78 and 50 kPa.

The results of the calculations with compacted pellet filling in the bevel are shown in Figures 6-8 to 6-13. Figure 6-8 shows the upwards displacement of different points above the canister. The figure shows that the maximum displacement of the buffer is 5.4 cm but the displacement of the top part of the backfill blocks in the deposition hole is larger or 7.1 cm. The figure also shows that the swelling has not come to complete stop due to convergence problems but also that the increase is slow and close to equilibrium at the end of the calculation (at 143 years). The calculation has thus been run much longer than for case 1, which is logical since the pellet filling is stiffer and the displacements smaller. However, there is also an influence of the damping forces that prolongs the time to equilibrium so the time evolution is not modelled in a correct way.

That the calculation has stopped before equilibrium is confirmed in Figure 6-9, which shows the pore pressure distribution at the end. The pore water pressure has decreased from the initial 7 MPa but to 300 kPa at some distant parts of the backfill and about 100 kPa close to the bevel, which is much better than for case 1 but still not completely in equilibrium.

Figure 6-10 and 6-11 shows contour plots of the upwards swelling at the end of the calculation. The figures show that in addition to the upwards swelling of the buffer and the backfill blocks in the deposition hole there is a downwards swelling of up to 5 cm of the backfill to the pellets filling in the bevel.

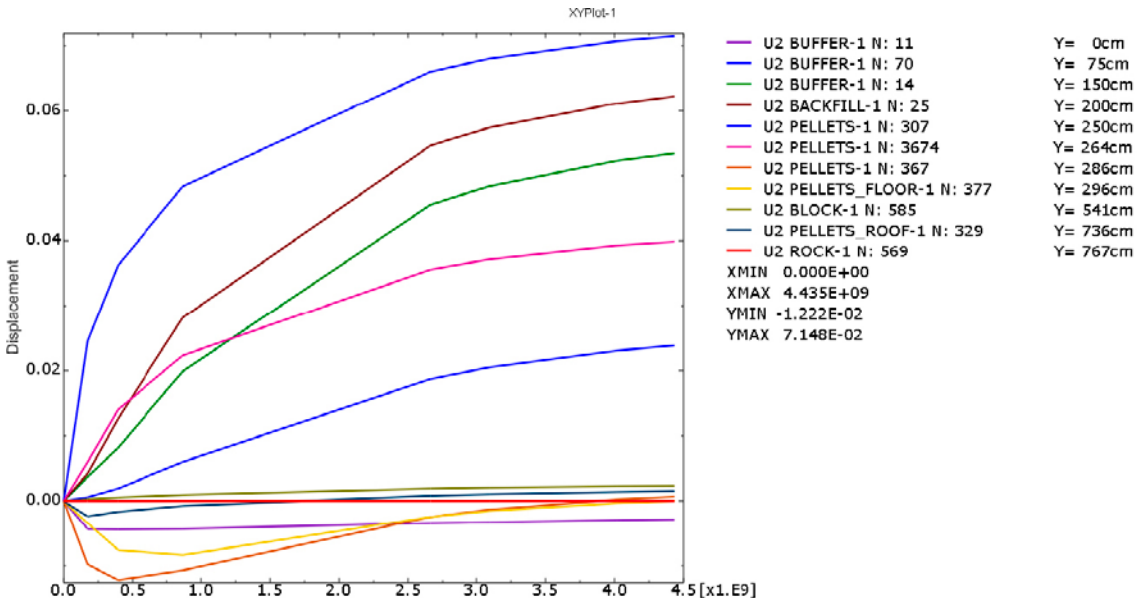

Figure 6-8. *Upwards displacements (m) vs. time (s) of different nodes in the vertical centre line of the deposition hole. Y = distance from canister top.*

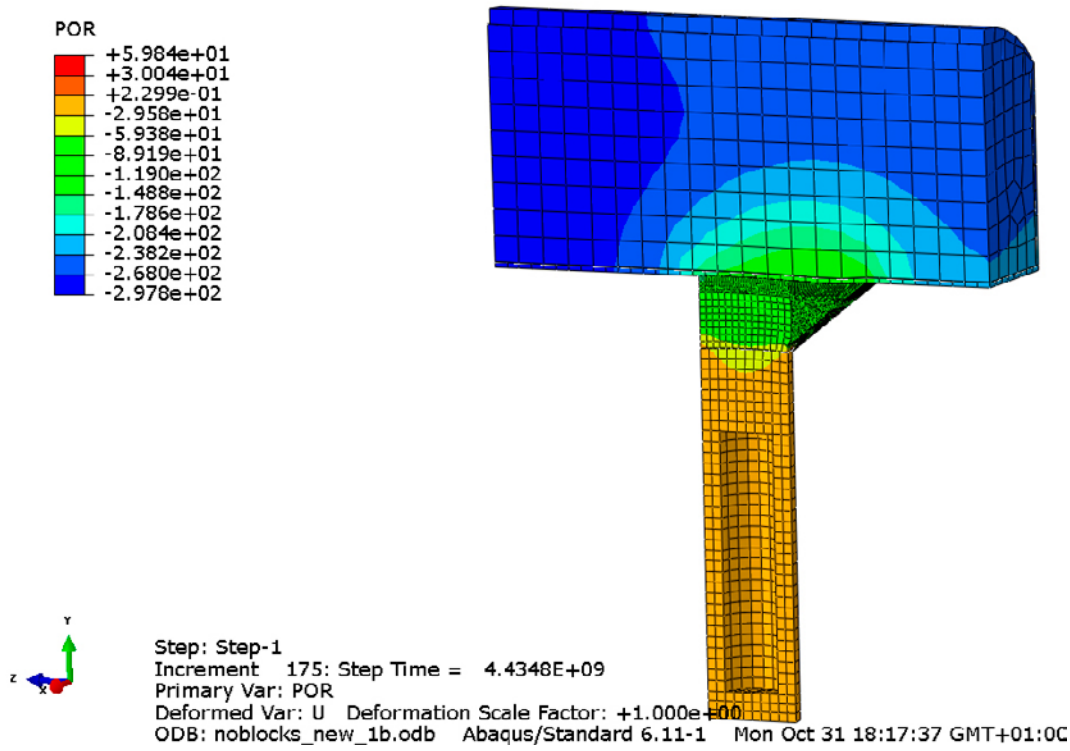

Figure 6-9. *Pore water pressure (kPa) distribution at the end of the calculation.*

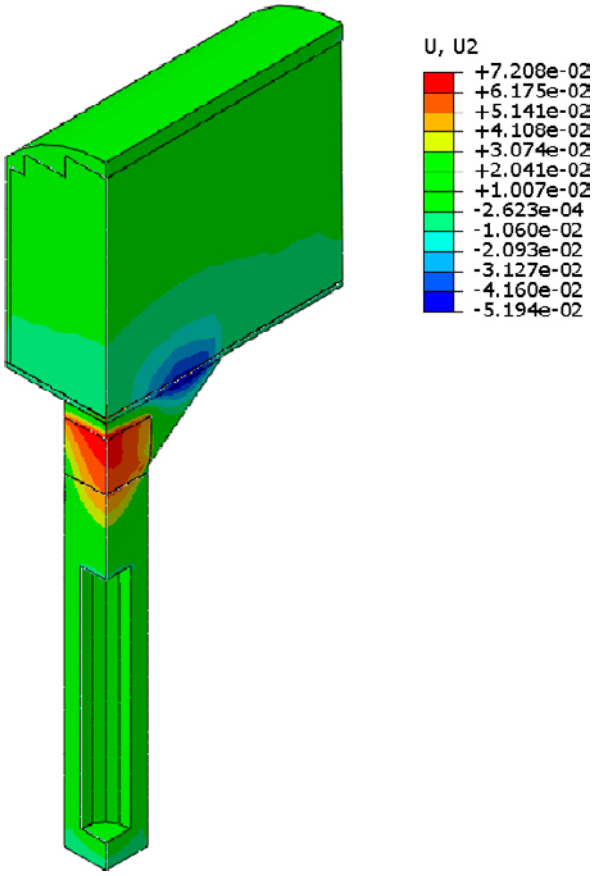

Figure 6-10. *Contour plot of the vertical upwards displacements (m).*

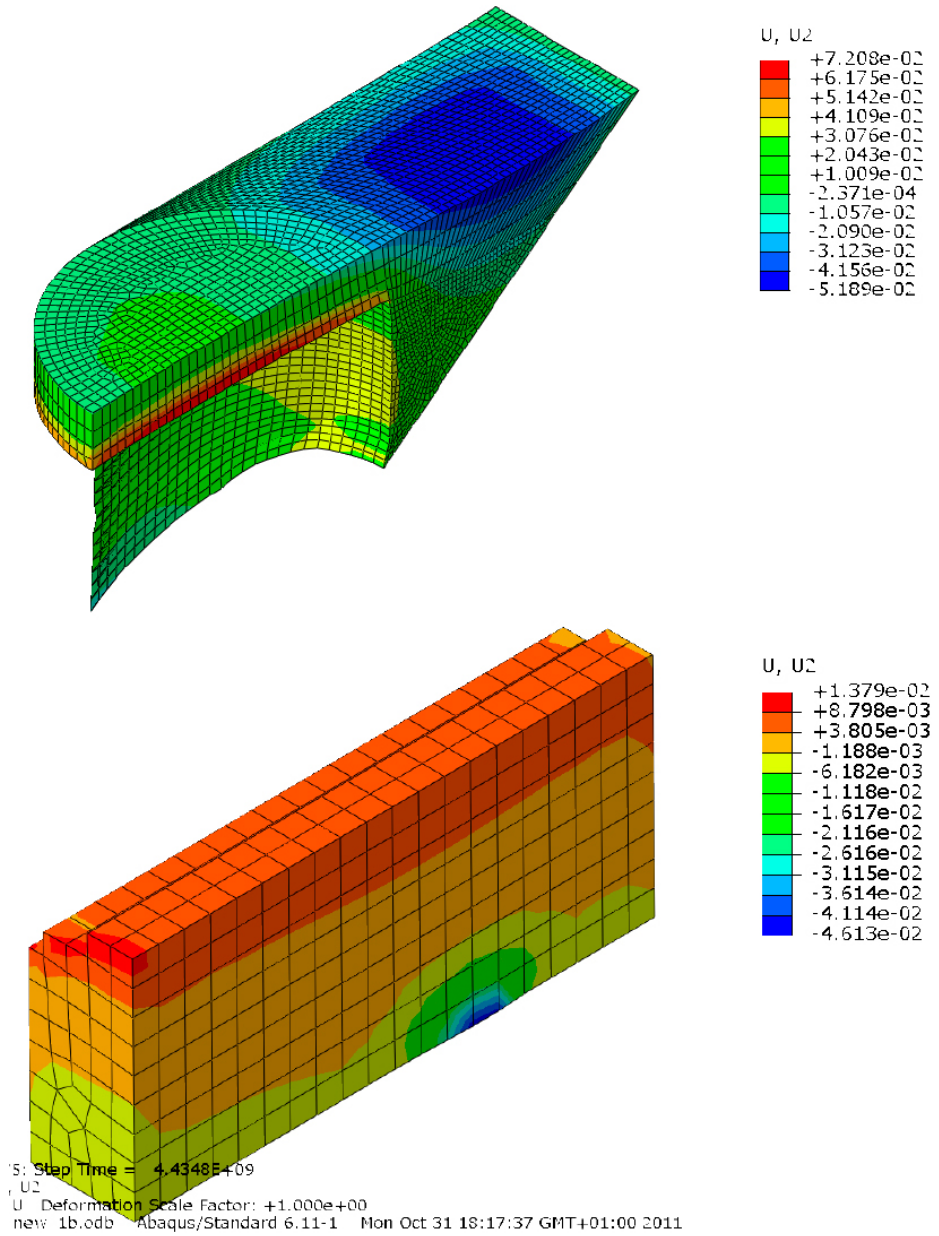

Figure 6-11. *Contour plots of vertical upwards swelling (m) of some details. The upper picture shows the pellets filled parts and the lower picture shows the backfill.*

Figure 6-12 shows the sideways swelling. The sideways swelling is quite large and the upper backfill blocks have swelled more than 9 cm into the bevel, which is still 6 cm less than for case 1.

The void ratio in the buffer is shown in Figure 6-13. The figure shows that the highest void ratio in the buffer above the canister is about 0.81, which corresponds to a density at saturation of 1,980 kg/m^3. This should be acceptable, even though the calculation was not run to full equilibrium. The figure also shows that the void ratio in the top of the buffer is uneven with high void ratio at some part. However the corner problems that caused a local very low void ratio around one node in case 1 is not seen in this calculation, which means that the calculation is probably more reliable (also considering that it has reached closer to equilibrium).

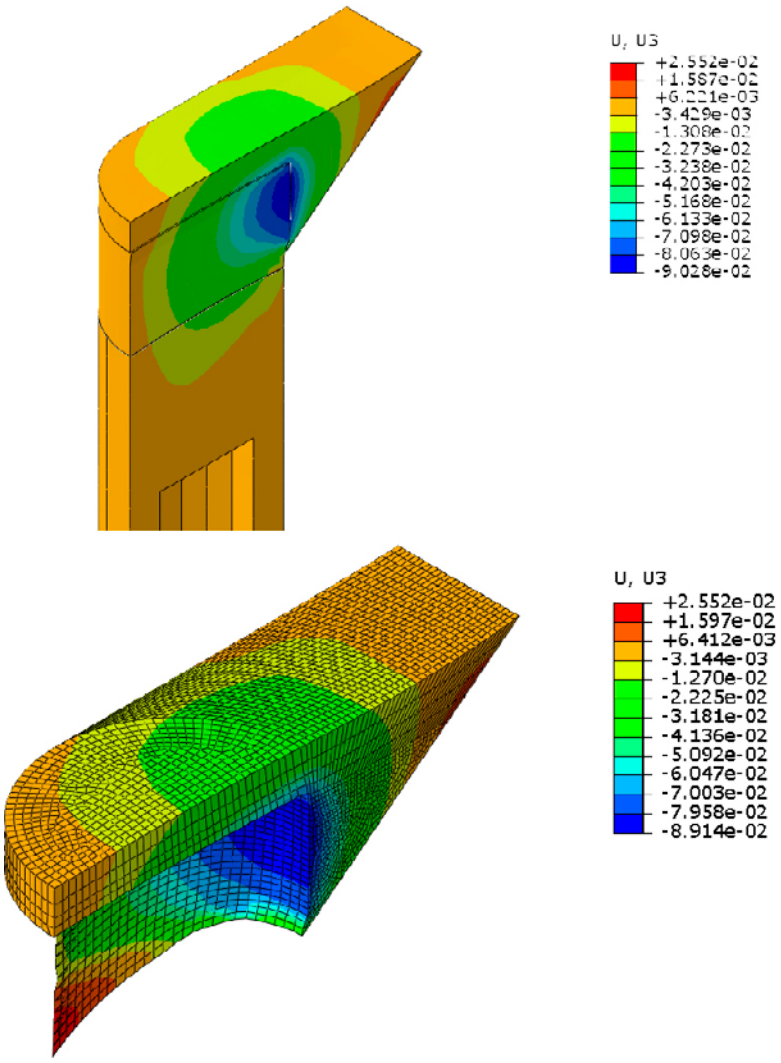

Figure 6-12. *Contour plots of the sideways displacements (m). Only the pellets filling in the bevel and the deposition hole is shown in the lower picture.*

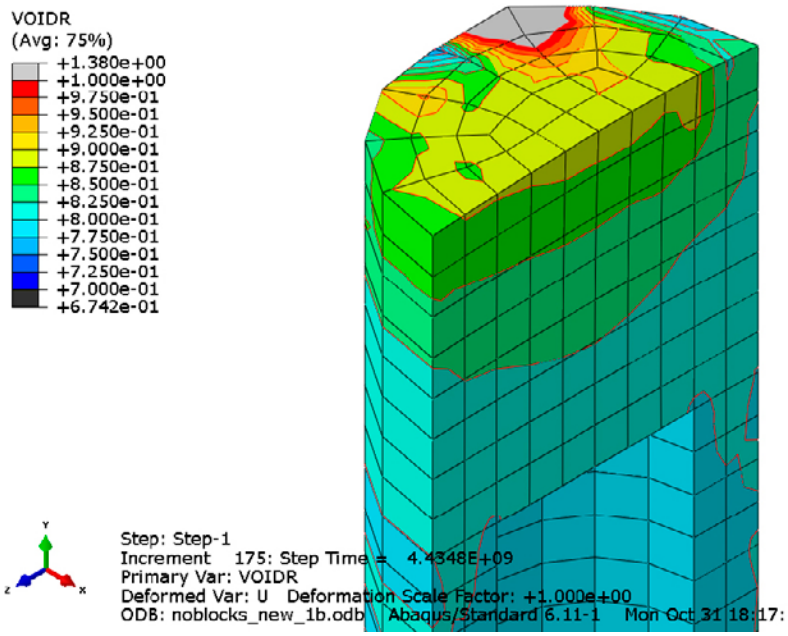

Figure 6-13. *Void ratio in the upper part of the buffer.*

6.7 Conclusions from the wet case calculations

Although only two calculations were done for the wet case 1B, some evaluation of the results can be done.

The upwards swelling of the buffer/backfill interface is predicted to be 9–10 cm in the case of uncompacted pellet filling in spite of that the backfill in the tunnel is modelled with the same properties as the buffer. The reason is the combined effect of the vertical compression of the bentonite pellets in the upper part of the deposition hole and the sideways swelling into the pellet filled bevel.

The resulting swelling of the buffer leads to an almost unacceptable low density at the top of the canister. Since the backfill is modelled in an optimistic way with a homogenised density that is higher than the expected density and a material (MX-80) with a swelling pressure higher than the reference backfill, the real swelling will be considerably higher. The conclusion must thus be that uncompacted pellets in the bevel cannot be used.

It is difficult to judge if well compacted pellet filling in the bevel is sufficient, especially if it is combined with decreased thickness of the pellet filling between the backfill blocks in the deposition hole and in the tunnel. Additional modelling is required in order to better determine where the limits are. It is however recommended not to change the reference design by replacing the upper half block in the deposition hole with pellets.

The overall conclusion is thus that pellet filling in the upper part of the deposition hole is not acceptable.

7 Half block on top of deposition hole – case 2

7.1 Introduction

The conclusion from the studies reported in Chapters 5 and 6 was that the upwards swelling and subsequent loss of buffer density on top of the canister was too strong to be acceptable when the half-block was replaced by pellets. Both the dry case and the wet case were modelled and found not to fulfil the criteria.

The thick pellet filling thickness in the top of the deposition hole was the main reason for the strong swelling. The reference design, where the pellets filling is replaced by a 36 cm thick highly compacted bentonite block, is therefore modelled and studied in this chapter. Figure 7-1 shows the model.

Two new analyses have been made in order to investigate if the reference design is acceptable:

Dry case

The dry case refers to a case where the buffer in deposition hole is assumed to be completely water saturated and may swell and compress the backfill that is assumed to be unaffected by water. The dry case is analysed by using the old results, see Chapter 5.

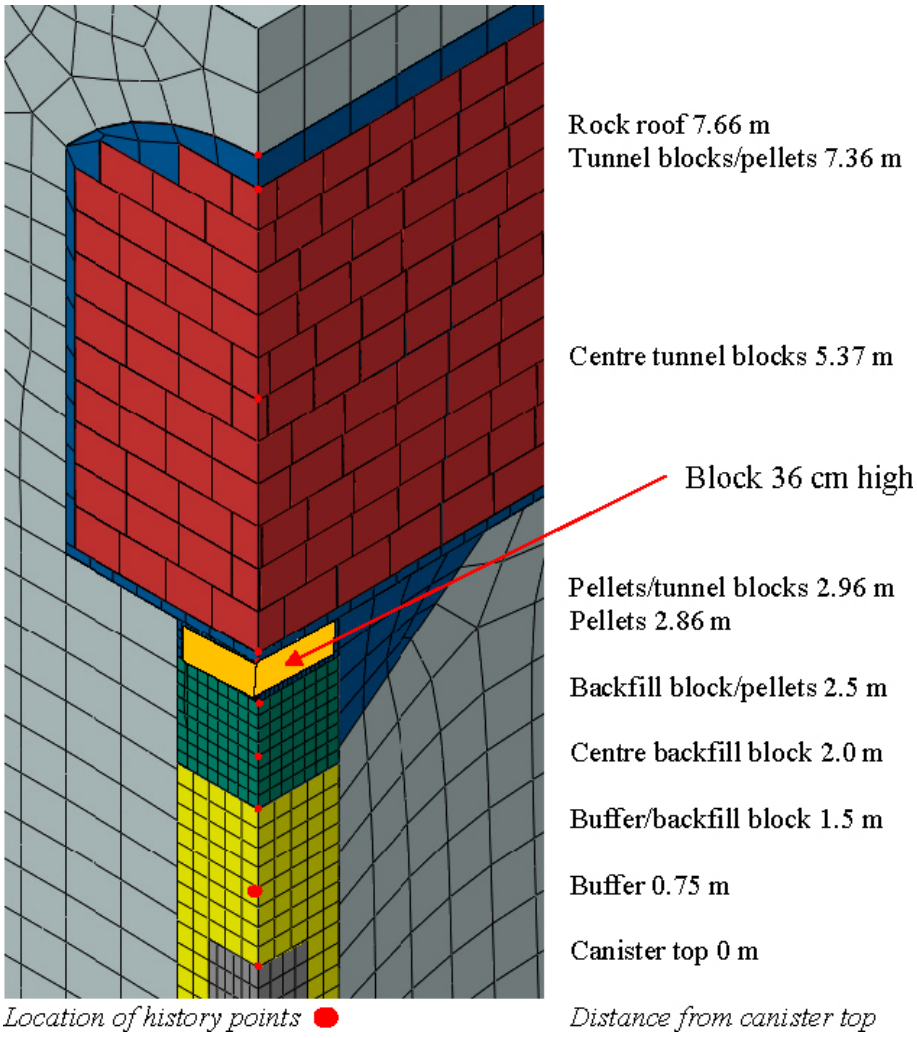

Figure 7-1. *Geometry and coordinates of the design analysed in Chapter 5 and 6 and an illustration of the proposed replacement of the pellet filling with a bentonite block.*

Wet case

The wet case refers to a case where both the buffer and the backfill, that is all bentonite parts, are water saturated and may swell and homogenise to steady state. The wet case is analysed with new finite element calculations.

7.2 Dry case (2A1)

The calculations were based on the modelling results shown in Chapters 5 and 6. In those calculations the 46 cm thick pellets filling had different stiffness with E- modules varying from 20 MPa to 3.9 MPa, the lower value representing loose pellet filling. The highest value 20 MPa is not realistic but was only made for evaluating a required simplification of the geometry.

In the reference design with a halfblock in the upper part of the deposition hole the pellet filling is 10 cm thick instead of 46 cm (in the alternative design), i.e. a factor 4.6 difference. The modelling with the unrealistically stiff pellet filling in the alternative design was made with E = 20 MPa, which is a factor 5.1 higher than E = 3.9 MPa that corresponds to loose pellet filling. The very stiff case in the alternative design should thus fairly well correspond to the reference design with a halfblock and loose pellet filling.

The average vertical stress in the bottom of the pellets filling (on top of the new block corresponding to the coordinate 2.86 m in Figure 7-1) is according to the results shown in Figure 5-8 about 2.1 MPa for this very stiff case. If this stress is used to calculate the expected compression of the pellet filling in the floor δ it will be

$$\delta = H \frac{\sigma}{M} \qquad 7\text{-}1$$

where

H = bed thickness (m)

σ = average vertical stress (MPa)

M = compression modulus

The relation between the compression modulus M and Young´s modulus E is

$$M = \frac{E(1 - v)}{(1 + v)(1 - 2v)} \qquad 7\text{-}2$$

where

v = Poisson´s ratio

Using E = 3.9 MPa and v = 0.3 the compression modulus will be M = 5.25 MPa and the compression

δ = 0.040 m

The compression 40 mm is almost identical to the compression of the pellet filling in the previous design with very stiff pellets (Table 5-5), which means that also the other parts of that calculation are likely to be valid, meaning that the expected buffer swelling will be about 90 mm and the expected density at saturation at the canister lid 1,950 kg/m^3. However, the E-modulus of the pellet filling in the roof is in this calculation very high (20 MPa), which means that the compression of this part will be larger if the E-modulus of uncompacted pellet filling E = 3.9 MPa is used and probably lead to a slightly too low density of the buffer.

The conclusion of the analysis is thus that the upwards swelling of the buffer will be too large even for this case with a pellets thickness of only 10 cm if the pellet filling is uncompacted. This conclusion is somewhat surprising considering that the thickness of the pellet filling is reduced with a factor of 4.6, but the reason is the high compressibility of the uncompacted pellet filling.

If the 10 cm pellet filling is compacted, the density criteria will most likely be fulfilled, which was also the conclusion in the older calculations with 8 cm thick compacted pellet filling in the floor (Börgesson and Hernelind 2009).

The conclusion from these simple calculations is thus that a pellet thickness of 10 cm will work, but only if the pellet filling is compacted.

7.3 Wet case (2B1)

7.3.1 General

The wet case needs to be modelled since it includes the triangular bevel, which could be neglected in the dry case.

The geometry is very complicated and the deformations large, which have resulted in that the modelling has been difficult and that the results achieved are not completely satisfactory since some elements were unrealistically deformed. However, the results are judged to be enough informative in order to be able to draw required conclusions.

7.3.2 Element mesh

The element mesh is shown in Figure 7-2. It is similar to the mesh used for corresponding calculations in Chapter 6. The difference is that 36 cm of the pellet filling in the top of the deposition hole is exchanged for a material with the same properties as the buffer material and that the pellet filling around the backfill is modelled as the pellet filling in the bevel.

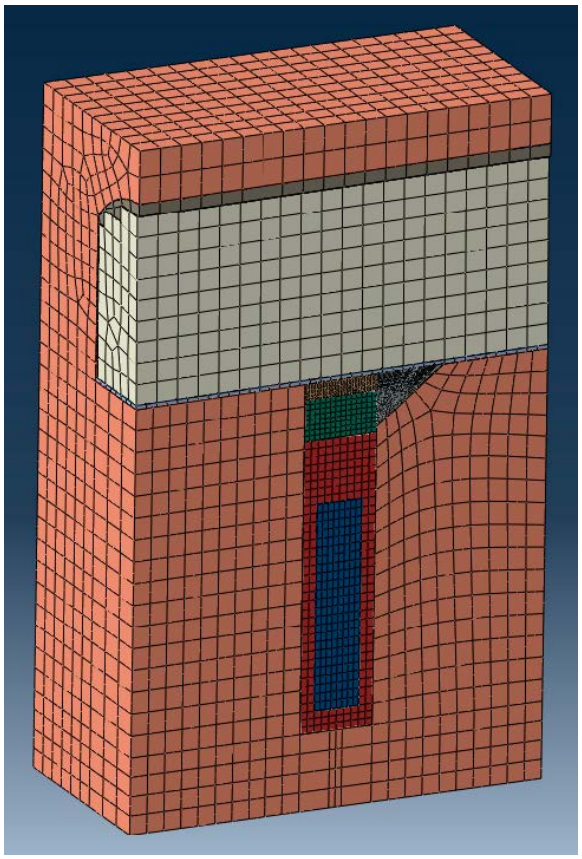

Figure 7-2. *Element mesh for the calculation of the wet case.*

7.3.3 Material properties

The bentonite parts are divided into two materials with very different initial density, namely high density bentonite and pellet filling. Both are modelled with pore pressure elements and as porous elastic materials with Drucker-Prager plasticity. The properties of those bentonite materials are identical to the properties of the buffer described in Section 5.3.1.

The materials and their initial conditions are as follows:

High density bentonite parts

The entire buffer and the bentonite block section of the backfill are modelled as completely water saturated and are assumed to have an average density at saturation of ρ_m = 2,000 kg/m^3 or the void ratio e = 0.77. The pore pressure is set to u = –7 MPa in order to correspond to the effective average stress p = 7 MPa that yields zero total average stress. The initial conditions of the buffer are thus:

u_0 = –7 MPa

p_0 = 7 MPa

e_0 = 0.77

Pellet filled parts

The pellet filling in the bevel and around the backfill is modelled as completely water saturated. The model is the same as the model of the high density parts but the initial conditions differ (identical to how the pellet filling in the buffer was modelled for CRT and SR-Site (Åkesson et al. 2010)):

u_0 = –50 kPa

p_0 = 50 kPa

e_0 = 1.78

This case corresponds to loose filling of the pellets (dry density 1,000 kg/m^3).

Other materials

The rock and the canister are modelled as very stiff linear elastic materials with no pore pressure elements.

Figure 7-3 shows the different materials.

The backfill model differs from the backfill model used in the calculations described in Chapter 6. That backfill model had no pellet filling, but had the same properties as the high density bentonite in the entire tunnel. The reason for changing the model is that the average dry density 1,560 kg/m^3 was too high (as mentioned in Section 6.3.2). Such high density corresponds to a degree of block filling in the tunnel of about 82% at the pellet filling dry density of 1,000 kg/m^3, which is higher than the expected average values. According to the production line report (SKB 2010) the average backfill dry density will range between 1,458 and 1,535 kg/m^3. The backfill used in the present calculations has an average dry density of 1,487 kg/m^3, which is in better agreement with expected. In addition, an initially inhomogeneous backfill is also in better agreement with the actual design. However, we still have a material model that assumes high montmorillonite content and thus high swelling pressure in relation to the acceptable montmorillonite content.

7.3.4 Boundary conditions and calculation sequence

Contact surfaces

The contacts between *the high density bentonite and the rock, the high density bentonite and the canister* and *the pellets filling and the rock* have not been tied in order to allow slip. Instead interface properties with a specified friction have been applied between the different materials. The friction has been modelled with Mohr Coulomb's parameter friction angle ϕ and without cohesion c.

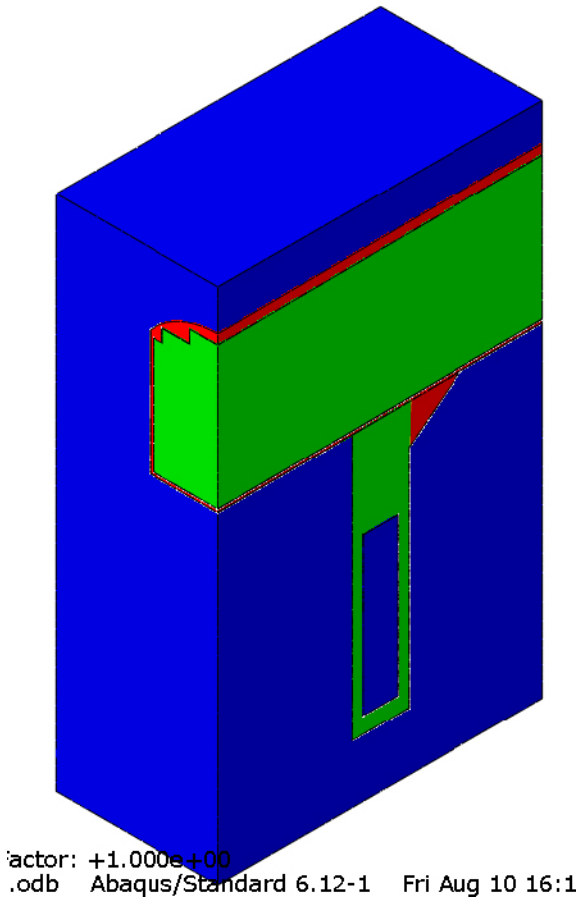

Figure 7-3. *Materials in the model. Green = high density bentonite, red = pellet filling, blue = other non-porous materials.*

The following basic value has been used for all density bentonite contacts:

$\phi = 8.69°$

$c = 0$

The contact surfaces are made not to withstand tensile stress, which means that the contact may be lost and a gap formed between the surfaces.

Another property of the contact surface is the so called “slip tolerance”, which describes the required slip to reach full friction. This parameter has been set to 0.005, which means that for the characteristic element length 0.2 m the contact works as an elastic spring when the slip is less than 1 mm.

Boundary and contact conditions

The following boundary and contact conditions are applied:

Mechanical

The vertical outer boundary planes are symmetry planes and free to move parallel with the plane and fixed perpendicular to the plane. The horizontal outer boundaries are fixed.

Hydraulic

All contacts between the rock and the bentonite (pellet filling and high density bentonite) have constant water pressure ($u = 0$ MPa), the contacts with the canister are no flow contacts and the vertical symmetry planes are no flow boundaries.

Calculation sequence

The calculations are coupled hydro-mechanical calculations. The pore water pressure in the hydraulic contacts between the bentonite parts and the rock is stepwise increased from –7 MPa to 0 MPa during 1,000 seconds. Then the actual consolidation calculation should run until complete pore water pressure equilibrium with pore pressure 0 MPa is reached in the entire bentonite. The calculation was run to 10^{11} seconds (more than 3,000 years) when almost complete pore pressure equilibrium was reached.

The calculations include a technique for facilitating the convergence conditions by introducing damping forces. This implies that the simulated time until pore pressure equilibrium is extended and that the time until the swelling is completed thus is not physical.

7.3.5 Results

The results after completed swelling and homogenisation are illustrated in Figures 7-4 to 7-7. Figure 7-4 shows the void ratio and Figure 7-5 shows the average swelling pressure. Figure 7-6 shows the vertical total displacements and Figure 7-7 shows the total horizontal displacements in the tunnel axis direction.

The results show that the influence of upwards swelling on the density of the buffer is very limited. Some observations:

The void ratio in the bevel is increased due to horizontal swelling of the bentonite in the deposition hole and vertical swelling of the bentonite in the tunnel. The highest void ratio in the bevel is still about $e = 1.2$ ($\rho_m = 1{,}810$). The void ratio above the canister is insignificantly decreased to about $e = 0.79$ ($\rho_m = 1{,}994$).

The average stress follows naturally the void ratio with a rather strong swelling pressure drop towards the rock surface in the bevel but an insignificant drop on top of the canister (to about 6.5 MPa).

The vertical displacements are rather strong around the bevel. The compression of the pellet filling in the bevel from the backfill is up to 15 cm, while the displacements of the upper surface of the extra block installed in the deposition hole is rather small or a few cm directed downwards (due to the horizontal swelling into the bevel).

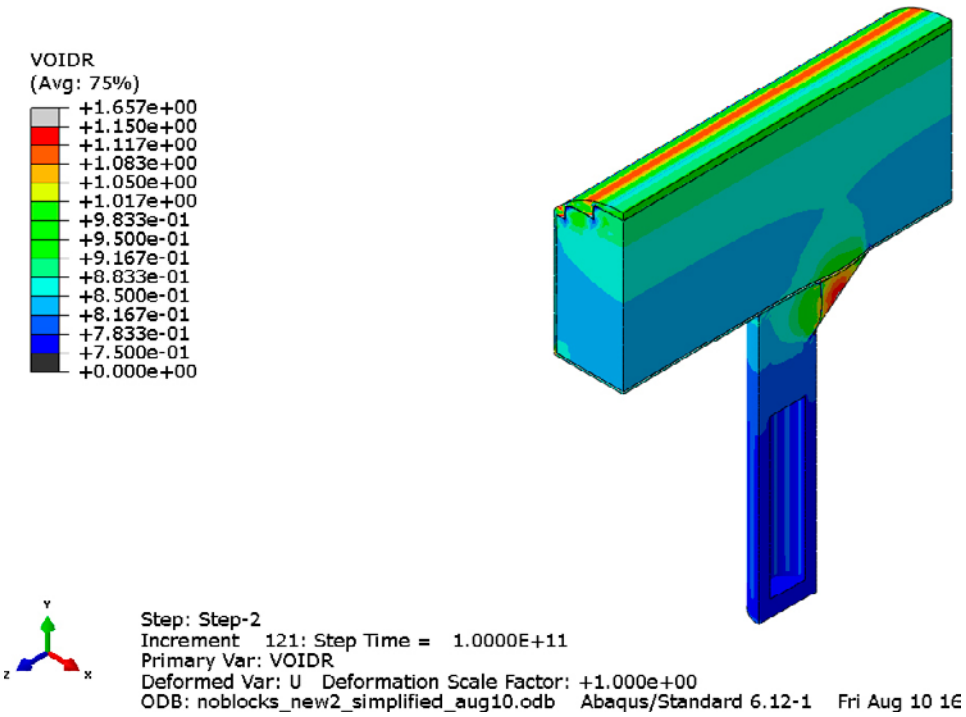

Figure 7-4. *Modelled final void ratio distribution.*

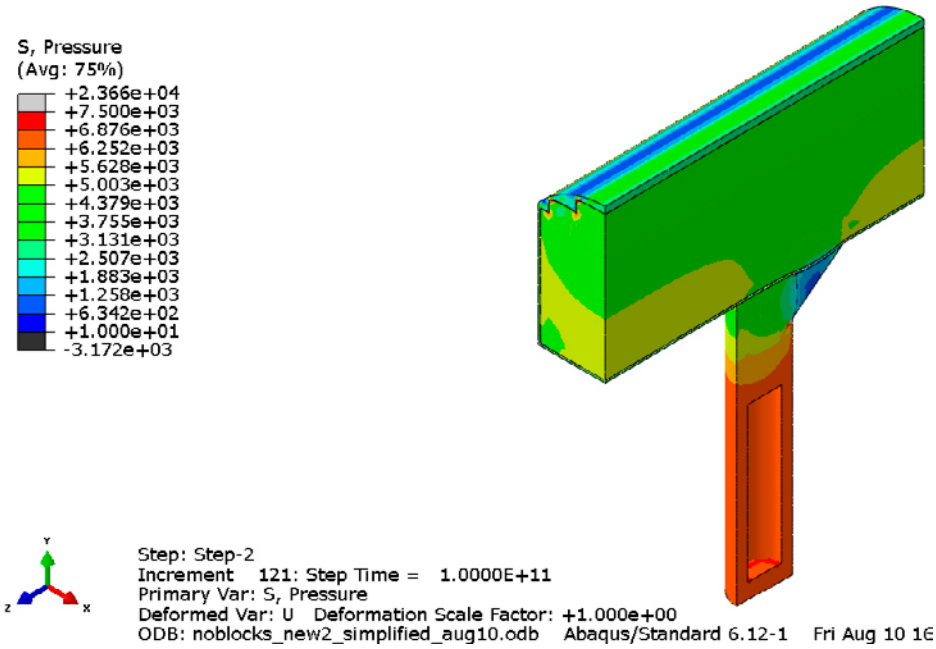

Figure 7-5. *Modelled final average distribution of swelling pressure (kPa).*

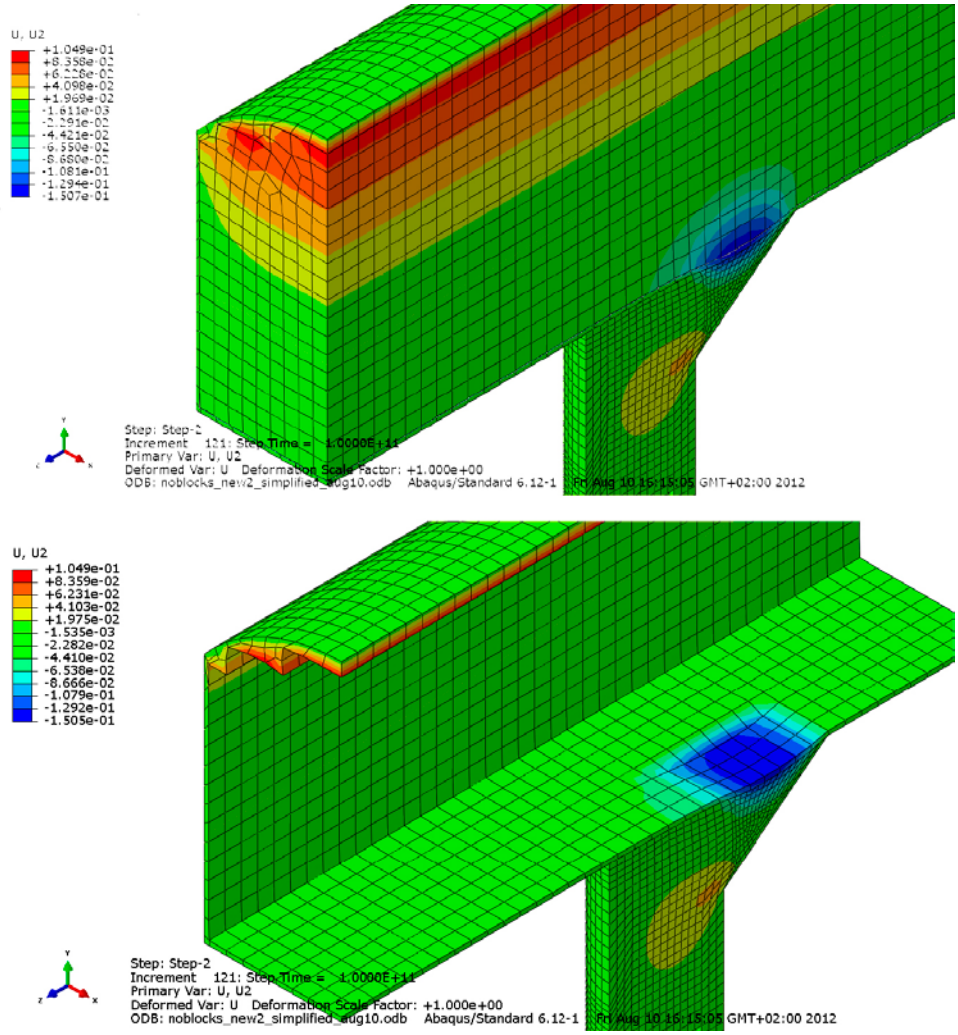

Figure 7-6. *Modelled final total vertical displacements (m). The originally high density backfill is removed in the lower picture.*

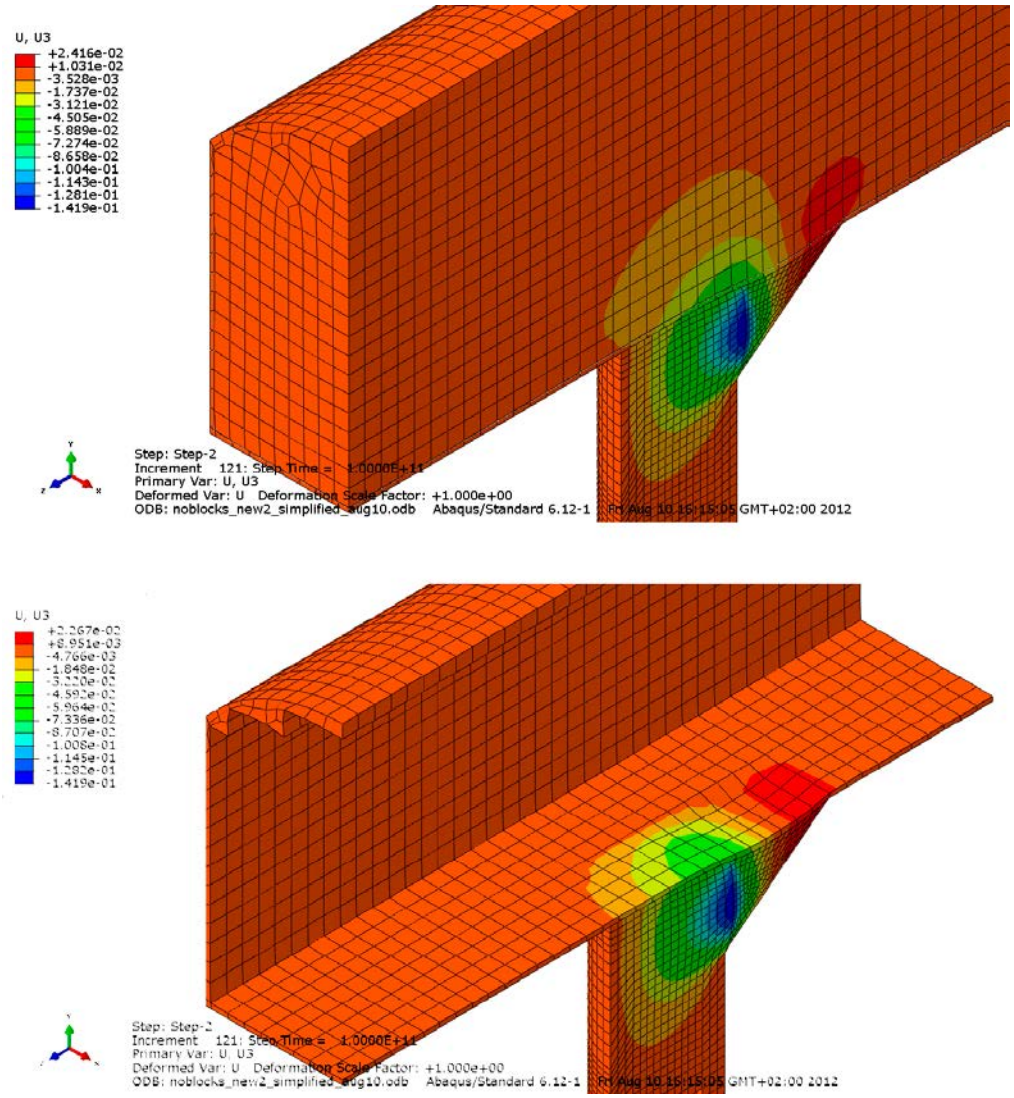

Figure 7-7. *Modelled final total horizontal displacements (m). The originally high density backfill is removed in the lower picture.*

The horizontal swelling in the direction of the tunnel axis is also very strong at the bevel (up to 14 cm).

The conclusion of the calculations is that the wet case with loose pellet filling is not a problem for the density of the buffer material above the canister.

7.4 Influence of having a bevel or not

In order to study the influence of the bevel calculations without bevel has been performed with the same geometry and materials as the reference design with a half block.

Dry case (2A2)

The two calculations of the dry case made with and without bevel in the design with pellet filling instead of half block (Section 5.6) showed insignificant difference (see Table 5-5). The pellet filling in this case had an unrealistic low compressibility in order to make the calculation with bevel converge. However, in the reference design the half block is dry just as the upper two blocks in the deposition hole, which means that there will be no lateral swelling into the pellet filled bevel. There are thus strong indications that there will be little or no influence of the bevel in the dry case.

The influence of the bevel if also the backfill blocks in the upper part of the deposition hole would be assumed to be wet has not been modelled. It is not obvious if this yields higher or lower final density of the buffer at the canister lid.

Wet case (2B2)

For the wet case there will be large lateral swelling into the bevel as shown in Section 7.3. Although the calculations showed that this case was acceptable with bevel it is valuable to compare the results when having a bevel or not.

A new model was worked out with identical geometry and properties as the model in Section 7.3, but with the bevel removed and replaced by solid rock. Figure 7-8 shows the model. Some results of the final vertical displacements and the void ratio distribution are shown in Figure 7-9.

The density at full saturation of the two cases with and without bevel is compared in Figure 7-10. The figure shows that the density on top of the canister as expected is slightly higher when there is no bevel, but the difference is small and the density at the top of the canister is well within the acceptable level for both cases. The density of the bentonite in the upper part of the deposition hole at the contact with the bevel is strongly reduced to below $\rho_m < 1{,}900$ kg/m^3, but that does not affect the density at the top of the canister very much.

Lowest density ρ_m at the top of the canister:

With bevel: $\rho_m \approx 1{,}992$ kg/m^3

Without bevel: $\rho_m \approx 2{,}000$ kg/m^3

In Figure 7-10 the density at saturation on top of the canister is higher than $\rho_m = 2{,}000$ kg/m^3 in the calculation without bevel. This is due to that the initial void ratio is $e_i = 0.77$, which corresponds to the density $\rho_{mi} = 2{,}006$ kg/m^3.

The influence of the bevel on the upwards swelling of the buffer and the final density on top of the canister is thus quite small. The impact is however significant in the backfill blocks closest to the bevel.

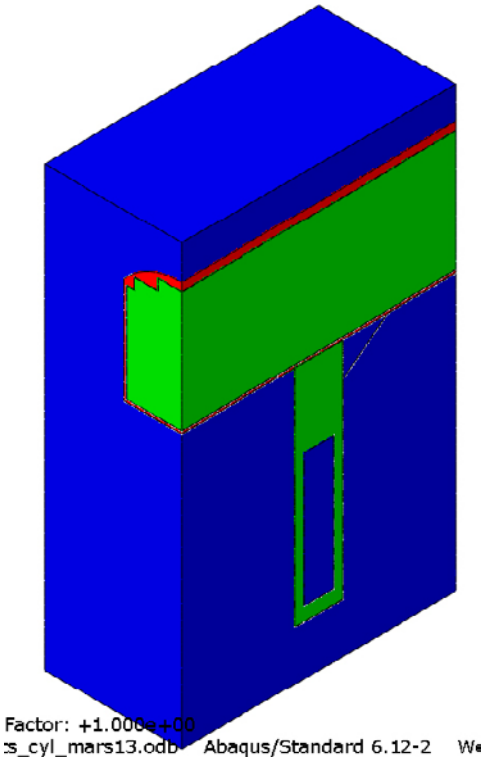

Figure 7-8. *Model without bevel. Materials in the model: Green = high density bentonite, red = pellet filling, blue = other non-porous materials.*

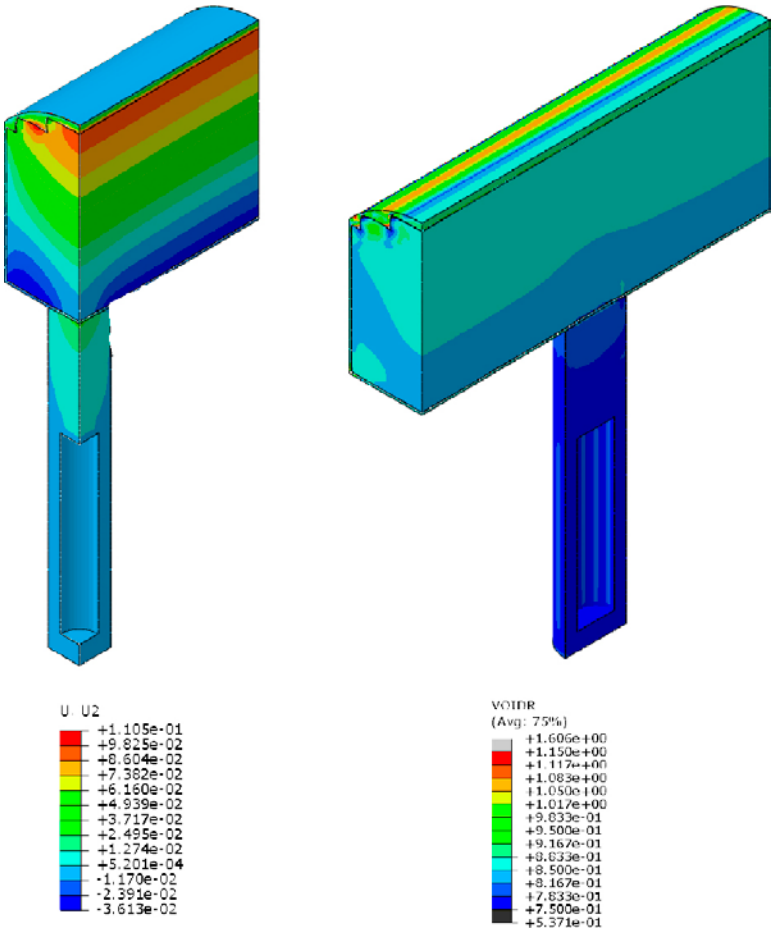

Figure 7-9. *Final vertical displacements U2 (m) and void ratio.*

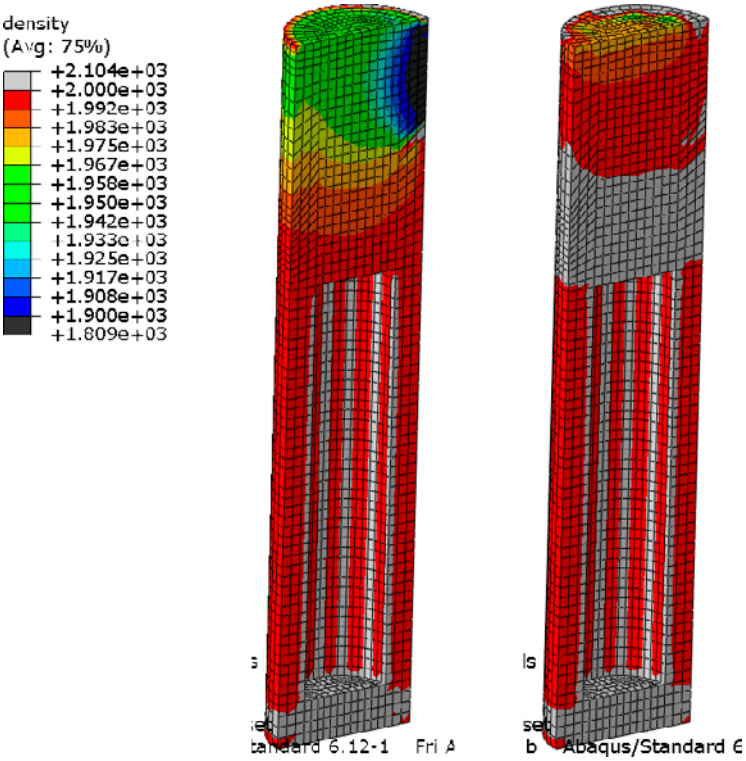

Figure 7-10. *Comparison of density at saturation (kg/m^3) in the entire deposition hole for the two cases with (left) and without bevel.*

8 Conclusions

Calculations of the upwards swelling of the buffer have been done for some variants of backfill design and with the bevel in the tunnel floor included.

With and without bevel and with pellet filling in the top of the deposition hole (case 1).

Three types of calculations of this case have been performed:

- Dry case
  - Dry backfill with different properties of the pellet fillings.
  - Dry backfill without pellet filling at the roof.
- Wet case
  - Completely water saturated backfill with bevel.

In spite of huge problems with convergence of the finite element calculations, some results that yield general conclusions were generated. The following conclusions can be drawn:

Dry case

The influence of the bevel is small but the small influence is entirely due to that the two backfill blocks in the deposition hole are assumed to remain dry. Since the influence is small most calculations were done without the bevel.

The stiffness and thickness of the pellet filling are the dominating properties regarding the influence on the upwards swelling and the subsequent density loss of the buffer. The results show that the design with pellet filling in the top of the deposition hole does not fulfil the requirements neither for uncompacted pellet nor for compacted pellet filling.

The calculations do not reveal what thickness of the pellet filling that can be accepted, but an estimate is that it needs to be halved if it is compacted since a double stiffness (extreme case) manages the density criterion.

The influence of the pellet filling at the roof is not very strong and the calculations imply that loose filling is acceptable but also that the pellet filling is needed and cannot be excluded.

Allowable thickness of the pellet filled slot at the roof depends of course on the other parameters (especially the pellet filling in the floor) but a rough estimate is that the compression of the pellet filling is about proportional to the thickness.

The influence of the backfill block section in the tunnel (and thus the horizontal joints between the blocks) is rather strong especially for those cases that are acceptable. It is thus important to learn more about the joint properties.

Wet case

The wet case was modelled with properties of the backfill identical to the properties of the buffer. This isolates the influence of the bevel alone but strongly underestimates the total upwards swelling

The influence of the bevel in the case of completely water saturated buffer and backfill is very strong in the sense that there is a significant lateral swelling of about 15 cm in the contact zone between the bevel and the backfill blocks. The reference design yields swelling that is just on the limit of acceptability of only the lateral swelling into the bevel. The conclusion is thus that the design with pellet filling in the top of the deposition hole is not acceptable with uncompacted pellets in the bevel.

It is difficult to judge if well compacted pellet filling in the bevel is sufficient, but it must then probably be combined with decreased thickness of the pellet filling between the backfill blocks in the deposition hole and in the tunnel. Additional modelling is required in order to better determine where the limits are.

Comments

The results lead to recommendations to reduce the thickness of the pellets filling between the backfill blocks in the deposition hole and the tunnel blocks to at least half and preferably one third (if uncompacted filling). They also lead to recommendations to use another filling of the bevel than pellets, e.g. compacted bentonite blocks that are fitted to the bevel.

With and without bevel and with half block in the top of the deposition hole (case 2)

By replacing the pellet filling with a block of highly compacted bentonite, as proposed for the reference design, the large swelling can be strongly reduced. This design has been investigated by calculating the buffer swelling at the two extreme cases dry and wet backfill with uncompacted pellet filling in the bevel and in the tunnel floor.

Dry backfill

This case was not modelled but analysed analytically with help of old results. The influence of the bevel is small since the blocks in the dry case do not interact with the pellet filling in the bevel. The results showed that this case could be acceptable if the 10 cm thick pellet filling was compacted but not if it was only loosely filled. The influence of the bevel is insignificant for this case.

Wet backfill

The wet case was modelled and the results showed that very little swelling and insignificant loss of buffer density occurred also if the pellet filling was uncompacted. Calculations with and without bevel were done and comparisons show that the influence of the bevel on the density of the buffer is not strong although also for this case there is a significant lateral swelling of about 15 cm.

The overall conclusion is thus that the dry case is critical and that the reference design with halfblock works if the 10 cm thick pellet filling above the deposition hole is compacted.

Remaining uncertainties

The calculations refer to two extreme cases of dry and wet backfill and completely wet buffer. It is not obvious that these cases are the most pessimistic although the dry case should yield the largest swelling of the buffer since the resistance from the backfill is without any swelling pressure.

The influence of the bevel if also the backfill blocks in the upper part of the deposition hole would be assumed to be wet has not been modelled. It is not obvious if this yields higher or lower final density of the buffer at the canister lid.

Another major uncertainty is the properties of the joints between the backfill blocks. Investigations of these properties are planned. A full scale test with the reference block configuration is planned to be installed in a tunnel in Äspö HRL. In conjunction with this test the compression properties of the block assembly will be tested with a pressurised plate that simulates swelling bentonite buffer in a deposition hole.

It should also be noted that a bentonite with the same properties as MX-80 is used as backfill material. If the lowest acceptable bentonite content is used the results with differ and yield more upwards swelling for the wet cases but not for the dry cases. A larger pellet filled slot at the roof will also increase the upwards swelling.

References

SKB's (Svensk Kärnbränslehantering AB) publications can be found at www.skb.se/publications.

Börgesson L, Hernelind J, 2006. Canister displacement in KBS-3V. A theoretical study. SKB TR-06-04, Svensk Kärnbränslehantering AB.

Börgesson L, Hernelind J, 2009. Mechanical interaction buffer/backfill. Finite element calculations of the upward swelling of the buffer against both dry and saturated backfill. SKB R-09-42, Svensk Kärnbränslehantering AB.

Börgesson L, Johannesson L-E, 2006. Consequences of upwards swelling from a wet deposition hole into a dry tunnel with backfill made of blocks. A preliminary study. SKB TR-06-12, Svensk Kärnbränslehantering AB.

Börgesson L, Johannesson L-E, Sandén T, Hernelind J, 1995. Modelling of the physical behaviour of water saturated clay barriers. Laboratory tests, material models and finite element application. SKB TR 95-20, Svensk Kärnbränslehantering AB.

Börgesson L, Fälth B, Hernelind J, 2006. Water saturation phase of the buffer and backfill in the KBS-3V concept. Special emphasis given to the influence of the backfill on the wetting of the buffer. SKB TR-06-14, Svensk Kärnbränslehantering AB.

Glamheden R, Fälth B, Jacobsson L, Harrström J, Berglund J, Bergqvist L, 2010. Counterforce applied to prevent spalling. SKB TR-10-37, Svensk Kärnbränslehantering AB.

Johannesson L-E, 2008. Backfilling and closure of the deep repository. Phase 3 – pilot tests to verify engineering feasibility. Geotechnical investigations made on unsaturated backfill materials. SKB R-08-131, Svensk Kärnbränslehantering AB.

Johannesson L-E, Nilsson U, 2006. Deep repository – engineered barrier systems. Geotechnical behaviour of candidate backfill materials. Laboratory tests and calculations for determining performance of the backfill. SKB R-06-73, Svensk Kärnbränslehantering AB.

Karnland O, Olsson S, Nilsson U, 2006. Mineralogy and sealing properties of various bentonites and smectite-rich clay materials. SKB TR-06-30, Svensk Kärnbränslehantering AB.

SKB, 2010. Design, production and initial state of the backfill and plug in deposition tunnels. SKB TR-10-16, Svensk Kärnbränslehantering AB.

Åkesson M, Kristensson O, Börgesson L, Dueck A, Hernelind J, 2010. THM modelling of buffer, backfill and other system components. Critical processes and scenarios. SKB TR-10-11, Svensk Kärnbränslehantering AB.